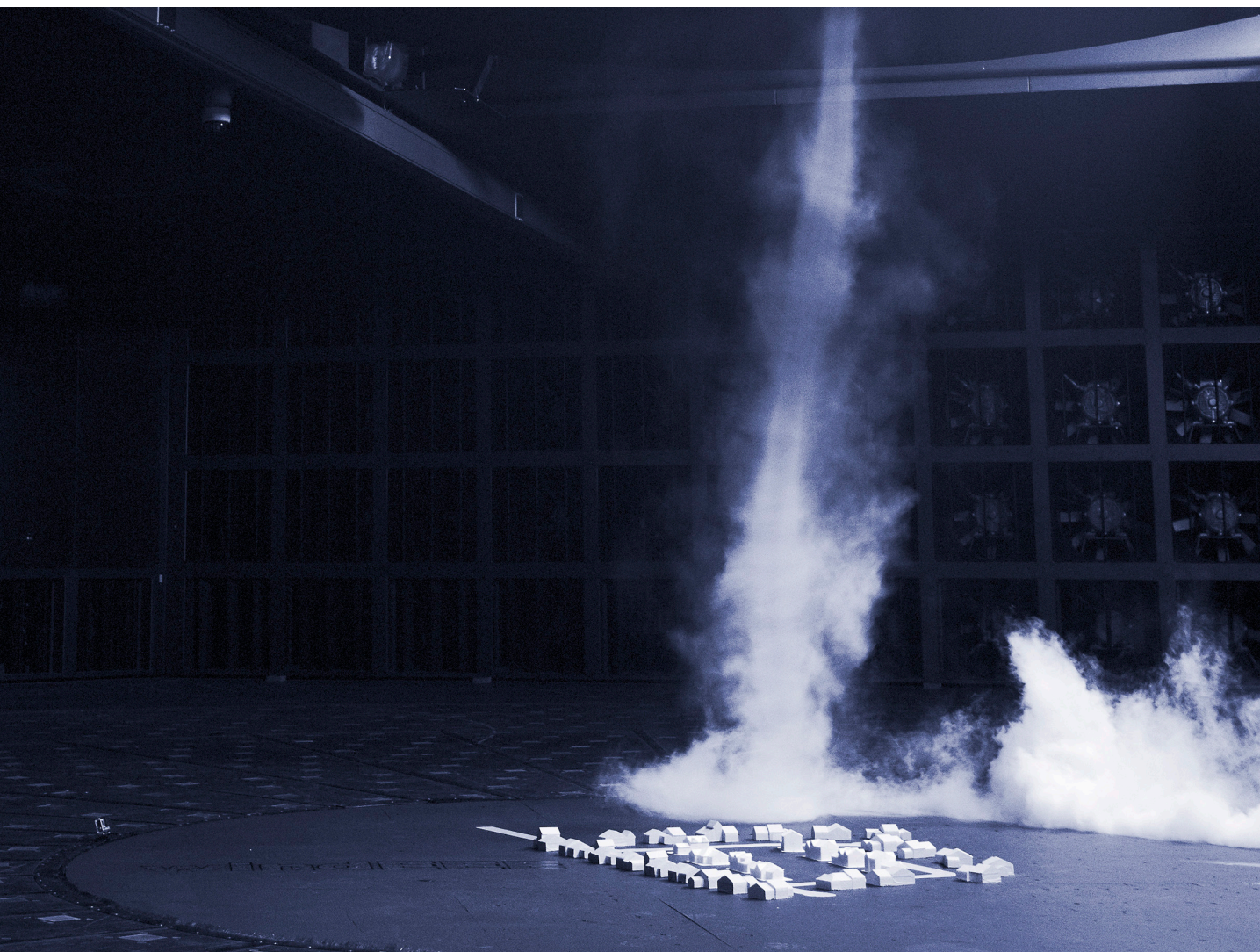


ANNUAL REPORT | 2018-2019



Western



WindEEE Research Institute
Engineering, Energy & Environment

© 2019 WindEEE Research Institute, Western University
2535 Advanced Avenue, London, Ontario, N6M 0E2, Canada

Production : Tristan Cormier, Elisa Yaquian

Printed and bound in Canada

Contents

PREFACE	5
GOVERNANCE STRUCTURE	7
PEOPLE	8
FACULTY	8
STAFF	8
INTERNATIONAL RESEARCH BOARD	9
ADVISORY BOARD	10
POSTDOCTORAL FELLOWS, GRADUATE AND EXCHANGE STUDENTS	11
FACILITIES AND EQUIPMENT	15
WINDEEE DOME	15
MODEL WINDEEE DOME (MWD)	15
TESTING CAPABILITIES	16
EXAMPLE USES	17
EQUIPMENT	17

FLOW PROPERTIES FOR A LARGE-SCALE TORNADO-LIKE VORTEX	19
COMBINED WIND AND ICE LOADING ON TRANSMISSION LINES	20
AERODYNAMIC LOADING OF A TYPICAL LOW-RISE BUILDING FOR AN EXPERIMENTAL STATIONARY AND NON-GAUSSIAN IMPINGING JET	21
FLOW FIELD DYNAMICS OF LARGE-SCALE EXPERIMENTALLY PRODUCED DOWNBURST FLOWS	23
THREE-DIMENSIONAL MEASUREMENTS OF TREE CROWN MOVEMENT USING KINECT	24
MODELING OF TORNADO-LIKE VORTICES: MEAN AND FLUCTUATIONS	25
SURFACE PRESSURE MEASUREMENTS UNDER TRANSLATING TORNADO-LIKE VORTICES	26
ENVIRONMENTAL IMPACTS OF HIGH INTENSITY WINDS ON COMMUNITIES	27
MONTE CARLO MODELLING OF TORNADO LOSSES ON RESIDENTIAL BUILDINGS	28
THREE-DIMENSIONAL, NON-STATIONARY AND NON-GAUSSIAN (3D-NS-NG) WIND FIELDS AND THEIR IMPLICATIONS TO WIND-STRUCTURE INTERACTION PROBLEMS	30
TRANSIENT BEHAVIOR IN IMPINGING JETS IN CROSSFLOW WITH APPLICATION TO DOWNBURST FLOWS	32
A NOVEL APPROACH TO SCALING EXPERIMENTALLY PRODUCED DOWNBURST-LIKE IMPINGING JET OUTFLOWS	34
INVESTIGATION OF ABRUPT CHANGES (CHANGEPOINTS) IN A THUNDERSTORM VELOCITY RECORD	36
DYNAMIC STRUCTURAL ANALYSIS OF SCALED LIGHTING POLE MODEL IN PHYSICALLY SIMULATED TORNADIC FLOW	38
EXPERIMENTAL INVESTIGATION OF TORNADO RESILIENCE FOR A MODERN COMMUNITY SITUATED IN KANSAS, UNITED STATES.	40
SIMULATING OPERATIONAL EXTREME CONDITION FOR HORIZONTAL AXIS WIND TURBINES BASED ON IEC STANDARD	41
DRONE ENABLED AUTOMATED URBAN TOPOLOGY AND AIRFLOW MODELING	42
A NUMERICAL STUDY ON THE EXTERNAL CONVECTIVE HEAT TRANSFER COEFFICIENT FOR BUILDINGS IN DIFFERENT URBAN LAND-USE DESIGNATION	43
HINDCASTING THE DAMAGE OF OTTAWA-GATINEAU TORNADO OUTBREAK OF SEPTEMBER 2018: A COMPUTATIONAL APPROACH	44
LES OF TTU BUILDING AND ITS COMPARISON TO BLWT TEST RESULTS	45
WINDOW CONFIGURATION OPTIMIZATION IN BUILDINGS	46
INCORPORATING IMPROVED COMPUTATIONAL WIND ENGINEERING INTO HYBRID TESTING OF WIND TURBINES	47
NUMERICAL INVESTIGATION OF THE OBSTRUCTED FLOW AND HEAT TRANSFER CHARACTERISTICS IN THE AIR CHANNEL OF A BUILDING INTEGRATED PHOTOVOLTAIC/THERMAL ENVELOPE SYSTEM	48
FINITE ELEMENT MODELLING OF LOW-RISE BUILDING RESPONSE TO TORNADO LOADS	49
BIM INTEGRATED SUSTAINABLE AND RESILIENT BUILDING DESIGN FOR NORTHERN CLIMATE	50
EFFECTS OF CITY GROWTH ON TALL BUILDING CLADDING FATIGUE	51
DYNAMIC ANALYSIS FOR A NEGATIVE-GAUSSIAN CURVATURE CABLE DOME	52
ANALYSIS OF MID-RISE TIMBER BUILDINGS	53
BEHAVIOR OF TRANSMISSION LINE STRUCTURES UNDER TORNADO-INDUCED WIND LOADS	54
NUMERICAL MODEL FOR ANALYSIS OF WIND TURBINES UNDER TORNADOES	55
ANGLE AND END TRANSMISSION LINES	56
TOWERS BEHAVIOR UNDER TORNADO WIND LOADS	56
PROGRESSIVE FAILURE OF SELF-SUPPORTED TRANSMISSION LINE TOWERS UNDER DIFFERENT TORNADO WIND FIELDS	57

SHEAR BUCKLING TESTING OF WOOD SHEATHING PANEL	58
DETAILED AND SIMPLIFIED NUMERICAL ANALYSIS OF MULTI- STORY LIGHT-FRAME WOOD BUILDINGS	59
BEHAVIOR OF WIND TURBINES UNDER DOWNBURST WIND LOADING	60
CASCADE FAILURE OF TRANSMISSION TOWERS ALONG A LINE SUBJECTED TO DOWNBURSTS.	61
ENVIRONMENT: BIOFIXATION OF CARBON DIOXIDE	62
OPTIMIZATION OF POROUS MEDIUM FOR SOLAR RADIATION CAPTURE	64
THE DEVELOPMENT OF AN OPTICAL GUIDE SYSTEM FOR PARABOLIC DISH SOLAR CONCENTRATORS	65
THE INFLUENCE OF WALL HEATING ON TURBULENT BURSTING AND SWEEPING PHENOMENA IN THE TURBULENT BOUNDARY LAYER	66
ENERGY MODELLING TO DETERMINE THE FEASIBILITY OF THERMAL REGULATION OF AQUACULTURE RACEWAYS BY UTILIZING GEOTHERMAL HEAT EXCHANGE	67
CHARACTERIZING THE FORMATION AND DYNAMICS OF LIQUID DROPLETS IN A GAS TURBINE AFTERBURNER-LIKE CONFIGURATION	69
CHARACTERIZING CONVECTIVE HEAT TRANSFER IN PCM-BASED LATENT THERMAL ENERGY STORAGE SYSTEMS	71
<u>PUBLICATIONS</u>	<u>72</u>
<u>CONFERENCES</u>	<u>74</u>
<u>GRANTS</u>	<u>77</u>
<u>HONORS AND AWARDS</u>	<u>79</u>
2019 HONORS AND AWARDS	79
2018 HONORS AND AWARDS	80
<u>EVENTS</u>	<u>82</u>
SHAD AT WINDEEE	82
WESTERN FORMULA RACING UNVEILING	83
<u>NOTES</u>	<u>84</u>

Preface

In June 2019, in accordance with the procedures laid out in the Manual of Administrative Policy and Procedures (MAPP), Section 7.9 for recognition of collaborative research entities at Western, the WindEEE Research Institute was re-approved for a three-year term by the VP Research. This is the third approval of WindEEE since its inauguration as an Institute in June 2011.

WindEEE RI is now maturing and the WindEEE Dome approaches the end of its IOF period estimated to end in 2021-22. Full attention is now paid to the operational phase, continuing with a high caliber research and industry projects as well as, towards the preparation for a new granting phase to ensure its future sustainability.

Moving forward, we have adopted 3 main strategic research priorities for the next 5 years (2019-2024):

- i. **Drive** *research* and *education* excellence and empower research teams so that they can pursue scientific investigation effectively in a world-class facility, the WindEEE Dome, and to develop real solutions for today's top wind engineering, wind energy and wind environment challenges;
- ii. **Enrich** the power of technology and *innovation* and extend collaborations to ensure that the novel infrastructure (WindEEE Dome) is optimally used by internal and external collaborators; and
- iii. **Grow** research through *sustainable* financial resources.

While we have defined these priorities for the next 5 years, we have already made significant progress on achieving these objectives. The following are evidence of this progress:

i/ During 2018-2019 fiscal year, the WindEEE RI core faculty group produced 39 international journal publications, 23 conference proceeding publications and 2.3M\$ in research funding. The core group faculty members at WindEEE RI have collectively

supervised 55 students (36 Ph.D; 18 M.Sc) as well as 9 Postdoctoral Fellows.

WindEEE RI, is currently co-hosting a 'Wind Research Seminar Series'. This is a monthly seminar series designed to enhance communication and collaboration among Western Engineering faculty, postdoctoral fellows, staff, and graduate students working on issues related to wind research.

Collaborative graduate programs are already in place with the Danish Technical University (DTU) and University of Genova (Italy), as well as with universities in South America through the CONACYT program. Other such programs are currently under development with Tongji University (China), Chongqing University (China), and the Polytechnic University of Bucharest (Romania). Based on these collaborations, Professor Giovanni Solari (University of Genova) and Professor Jakob Mann (DTU) have lectured graduate summer courses in 2017 and 2018 at Western University. The presence of these top international researchers enriches the educational and research activities at Western Engineering and at Western, in general. Their courses, together with the graduate courses taught by our best and brightest, are part of the Graduate Program in Wind Engineering which is one of the only two existing programs worldwide.

ii/ To expand its pan-Canadian research base, WindEEE RI in consultation with Research Services at Western, has dedicated a limited IOF-based funding, to invite researchers from across Canada to apply for a WindEEE Innovation Fund which is meant to provide researchers across Canada with competitive access to the WindEEE RI facilities to prove innovative concepts in wind research. New partnerships have been developed with Ocean Network Canada (ONC), University of Victoria (UVic), University of Windsor while we continue extending our collaboration with the Wind Energy Institute of Canada (WEICan), and UTIAS at University of Toronto.

At the international level, several research programs have been completed or are under development with partners from Europe, Americas and Asia. In collaboration with these partners, WindEEE has now

secured international research funding from prestigious agencies such as the European Research Council, the National Institute for Standards and Technology (NIST- USA), and Project 111 (China).

Since 2015, WindEEE is recognized by the Group of Senior Officials (GSO) as part of Global Research Infrastructures, a dedicated closed working space established by the European Commission called CIRCABC on which it started collaborating with global members. In 2016, WindEEE RI has become a member of SATA, the world Subsonic Aerodynamic Testing Association. In 2018, WindEEE has been invited to present its activities at the International Conference of Research Infrastructures held in Vienna, Austria under the auspices of the European Research Council. Thus, this international visibility and global impact has enabled WindEEE RI to be on the world map and be positioned as the “institute-of-choice” in the area of wind engineering.

iii/ The WindEEE RI Governance Structure has been amended to better reflect the nature of operations and funding to include: 1) The *Advisory Board* whose efforts are dedicated to Industry Partners and 2) a newly formed *International Research Board* to better reflect the high level of international interest manifested in WindEEE. Meanwhile the Canadian Research Membership has been extended and has increased its membership of more than 20 researchers from Western (out of 48 total pan-Canadian members), hosted in 3 departments of the Faculty of Engineering (Civil, Mechanical and Electrical Engineering) as well as Faculty of Science (Earth Sciences and Geography) and the Ivey School of Business.

Both the Research and Industry Funded Research projects at WindEEE RI continue to increase. R&D contracts with the insurance industry have been extended and are presently matched through NSERC CRD and OCE applications. Collaborations with transmission lines companies are presently expanding. A large research program with the NIST and Applied Research Associates Inc. (ARA-US) has been completed. A new European Research Council (ERC) funding program is unfolding, and a new

collaboration with the Institute for Catastrophic Loss Reduction has been developed.

These research priorities, as described above, are enabling all strategies to align with and support each other towards creating a world class research environment. With sustained growth, the Institute continues to strive to accomplish its Vision: ***to be a global leader in wind research and innovation.***



Horia Hangan
December 2019
London, Canada

Governance Structure

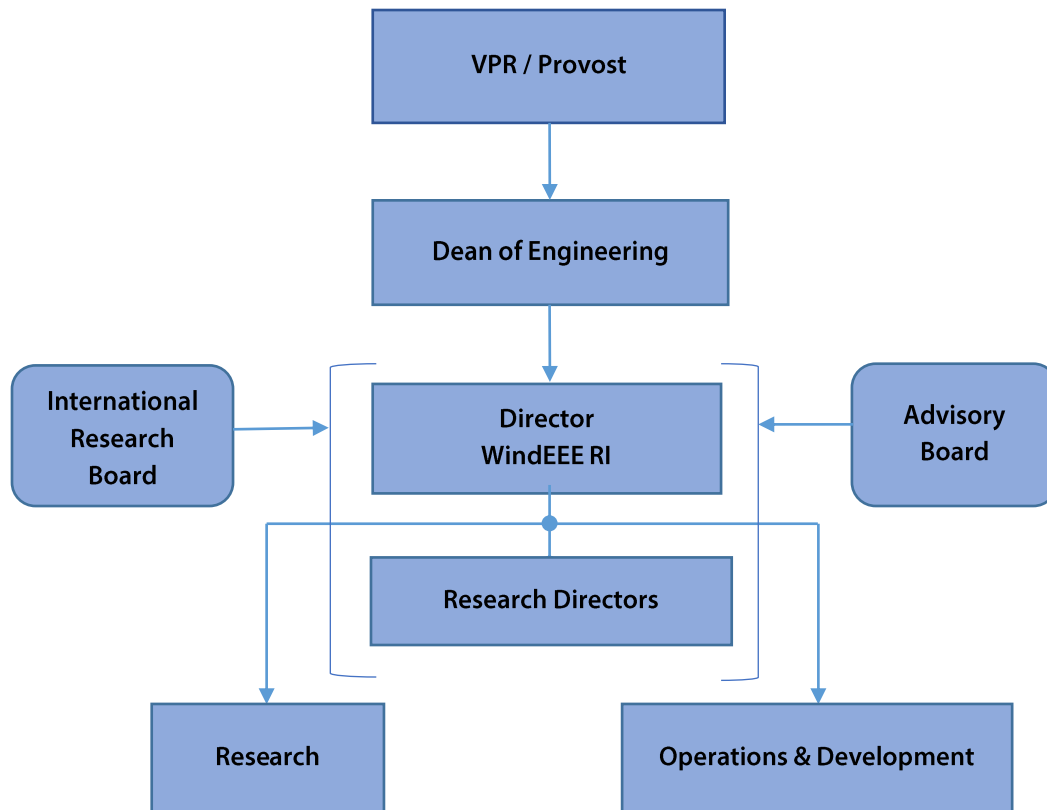
The **Governance Structure** provides both internal and external direction, innovative input and expert advice to the Institute in order to facilitate its development at Western and towards a National and International Institute, see the figure below. Two external Boards provide the necessary inputs to the Director of the Institute: The Advisory and the International Research Boards.

The **Advisory Board** (AB) advises the Director of the Institute on progress and advancement in areas related to WindEEE activities. The board reports on Industry, International Institutes and Government with a global perspective along with providing advice on potential sources of funding.

Since 2014, the Advisory Board meets once a year and Members from Industry, and Government organizations are nominated for three (3) year terms. They are listed in WindEEE RI Advisory Board.

The **International Research Board** (IRB) advises the Director and the Research Directors on the progress and advancement of the wind engineering, energy and environment sectors, with a scientific perspective. The International Research Board meets once a year and reviews the research activities of the Institute.

The Members of the International Research Board of the WindEEE RI are nominated for three (3) year term. They are listed in WindEEE RI International Research Board.



People

Faculty

Horia M. Hangan
Professor and Director of WindEEE Research Institute

Girma T. Bitsuamlak
Associate Professor and Research Director WindEEE Research Institute

Ashraf A. El Damatty
Professor and Research Director WindEEE Research Institute

Hassan Peerhossaini
Professor and Research Director WindEEE Research Institute

Kamran Siddiqui
Professor and Research Director WindEEE Research Institute

Staff

Jubayer Chowdhury
Adjunct Research Professor and Research Scientist WindEEE Research Institute

Tristan Cormier
Research Engineer

Adrian Costache
Operations Manager

Gerald Dafoe
Technical Specialist

Elisa Yaquian
Administrative Assistant

International Research Board

Rebecca Barthelmie
Professor, Cornell University, USA

Mark N. Glauser
Professor, Syracuse University, USA

Horia M. Hangan
Professor and Director of WindEEE Research Institute

Lord Julian Hunt
Former CEO and Professor, Met Services UK and Cambridge University, England

Ahsan Kareem
Director Natural Hazard Laboratory, Notre Dame University, USA

Mark Levitan
Lead, National Windstorm Impact Reduction Program R&D, NIST, USA

Jakob Mann
Professor, Danish Technical University, Denmark

Jonathan Naughton
Director Wind Energy Center, University of Wyoming, USA

Emil Simiu
NIST Fellow, National Institute of Standards and Technology, USA

Alexander Smits
Professor, Princeton University, USA

Giovanni Solari
Professor, University of Genova, Italy

Yukio Tamura
Professor, Tokyo Polytechnic University, Japan

You-Lin Xu
Professor, The Hong Kong Polytechnic University, China

Advisory Board

Hanny Hassan

Advisory Board Chair / President, Alef Consulting Inc., Canada

Mark Daley

Advisory Board Vice-Chair / Associate VPR, Western University, Canada

Hosam Ali

VP Research Area Director, Factory Mutual Global, USA

Anthony Ciccone

Principal, Power Sector, Golder Associates, Canada

Paul Dugsin

Managing Partner, Magnus Associates, Canada

Jon Galsworthy

VP, Canada Operations, Jensen Hughes, Canada

Horia M. Hangan

Professor and Director of WindEEE Research Institute

David A. Hickey

CEO Siemens Wind Power Ltd, Siemens Gamesa, Canada

Paul Kovacs

Executive Director, Institute for Catastrophic Loss Reduction, Canada

Scott Thomas

VP Risk Services, Zurich Insurance, Canada

Postdoctoral Fellows, Graduate and Exchange Students

Dr. D. Romanic – Postdoctoral fellow, Supervisor: Dr. H. Hangan
Dynamics of thunderstorm winds

A. Ashrafi – PhD candidate, Supervisor: Dr. H. Hangan
Experimental simulation of tornadoes and scaling properties

M. Enus – PhD candidate, Supervisor: Dr. H. Hangan
Development of large scale particle tracking methods

A. Gairola – PhD candidate, Supervisors: Dr. G.T. Bitsuamlak and Dr. H. Hangan
Numerical and WindEEE modeling of tornado flow structure and its effect on communities

M. Karami – PhD (completed), Supervisor: Dr. H. Hangan
Extraction of coherent structures from tornado-like vortices via POD method

A. Kassab – PhD candidate, Supervisor: Dr. H. Hangan
Simultaneous pressure and PIV measurements on low-rise buildings

E. G. Narancio – PhD Student, Supervisor: Dr. H. Hangan
Environmental impacts of high intensity winds on communities

J.P. Ortiz – PhD Student, Supervisor: Dr. H. Hangan
Non-synoptic wind effects on wind turbines

J. Chowdhury – MEng (completed), Supervisor: Dr. H. Hangan
Urban storm resilience

D. Davalos Arriaga – MEng Student, Supervisor: Dr. H. Hangan
Combined wind and ice loading on transmission lines

K. Shirzadeh Ajirlo – MEng Student, Supervisor: Dr. H. Hangan
Simulation of operational extreme conditions for horizontal axis wind turbines based on IEC standard

Dr. Z. Boutanios – Postdoctoral Fellow, Supervisor: Dr. G.T. Bitsuamlak
Computational wind engineering

Dr. A. Elshaer – Postdoctoral Fellow, Supervisor: Dr. G.T. Bitsuamlak
Computational wind engineering.

Dr. A. Ibrahim – Postdoctoral Fellow, Supervisor: Dr. G.T. Bitsuamlak
Computational wind engineering

Dr. M. Kaysay – Postdoctoral Fellow, Supervisor: Dr. G.T. Bitsuamlak
CFD model development for wind engineering and building science application

K. Adamek – PhD Student, Supervisor: Dr. G.T. Bitsuamlak
Adaptive Architectural Forms and Progressive Aerodynamics

T. Alemayehu – PhD Student, Supervisor: Dr. G.T. Bitsuamlak
Drone enabled environmental fluid mechanics modeling

A. Awol – PhD Candidate, Supervisors: Dr. G.T. Bitsuamlak and Dr. F. Tariku (BCIT, Canada)
Enhanced building energy performance evaluation

M. Ayalew – PhD Candidate, Supervisor: Dr. G.T. Bitsuamlak
Performance based wind design frame work for tall mass timber buildings

T. Berhane – PhD Candidate, Supervisor Dr. G.T. Bitsuamlak
Aerodynamic optimization of horizontal (bridge) structures

A. Gairola – PhD Candidate, Supervisors: Dr. G.T. Bitsuamlak and Dr. H. Hangan
Numerical and WindEEE modeling of tornado flow structure and its effect on communities

T. Geleta – PhD Candidate, Supervisor: Dr. G.T. Bitsuamlak
Performance based design framework for tornado

C. Howlett – PhD Student, Supervisor: Dr. G.T. Bitsuamlak
Aero-structural optimization of tall buildings

E.R. Lalonde – PhD Candidate, Supervisors Dr. G.T. Bitsuamlak and Dr. K. Dai (Tongji University, China)
Hybrid numerical and experimental wind and earthquake modeling

A. Melaku – PhD Candidate, Supervisor: Dr. G.T. Bitsuamlak
CFD based aeroelastic analysis of tall buildings

B. Nighana – PhD Candidate, Supervisor: Dr. G.T. Bitsuamlak and Dr. F. Tariku (BCIT, Canada)
Solar thermal and phase material integration with building envelope

M. Younis – PhD Student, Supervisor: Dr. G.T. Bitsuamlak
BIM integrated sustainable and resilient building design frame work

H. Abdallah – MEdSc Student, Supervisor: Dr. G.T. Bitsuamlak
City growth impact (urban topology change) on the design wind load

S. Laventure – MEdSc Student, Supervisor: Dr. G.T. Bitsuamlak
Wind induced response system identification

M. Sparks – MEdSc Student, Supervisor Dr. G.T. Bitsuamlak
Novel aeroelastic testing method development at WindEEE Dome

C. Van Der Kooi – MEdSc Student, Supervisor Dr. G.T. Bitsuamlak
Wind performance of tall mass timber buildings.

H. You – MEng Student, Supervisor: Dr. G.T. Bitsuamlak
A.I. Assisted Building Design

A. Ibrahim – Postdoctoral fellow, Supervisor: Dr. A.A. El Damatty
Analysis of wind turbines under tornadoes and downbursts

E. Abelraouf – PhD Student, Supervisor: Dr. A. A. El Damatty
Behaviour of curved roofs under wind loads

N. El Gharably – PhD Candidate, Supervisor: Dr. A. A. El Damatty and Dr. S. Easa (Ryerson University, Canada)
Application of supply chain demand in transportation engineering

A. Enajar – PhD Candidate, Supervisor: Dr. A. A. El Damatty
Nonlinear modeling of retrofitting systems of wood houses under uplift wind

N. Ezami – PhD Candidate, Supervisor: Dr. A.A. El Damatty
Testing of transmission line structures under tornadoes

M. A. Gazia – PhD Candidate, Supervisor: Dr. A.A. El Damatty and Dr. K. Dai (Tongji University, China)
Behavior of Extra Tall Wind Turbines under Extreme Load Events

M. Hamada – PhD Candidate, Supervisor: Dr. A.A. El Damatty
Analysis and testing of transmission lines under tornadoes wind

I. Ibrahim – PhD Student, Supervisor: Dr. A.A. El Damatty
Modelling and testing of progressive failure of transmission line structures

S. Maheux – PhD Candidate, Supervisor: Dr. A.A. El Damatty
Non-linear flutter behavior of cable-stayed bridges

M. Niazi – PhD Candidate, Supervisor: Dr. A.A. El Damatty
Performance of multi-story wood building under lateral loads

M. Ramadan – PhD Candidate, Supervisor: Dr. A.A. El Damatty and Dr. K. Dai (Tongji University, China)
Performance of wind turbines under tornados and downbursts

C. Santos – PhD (Completed), Supervisor: Dr. A. A. El Damatty and Dr. M. Pfeil (University of Rio De Janerio, Brazil)
Optimization of cable-stayed bridges considering wind loads

A. Shehata – PhD Candidate, Supervisor: Dr. A.A. El Damatty
Failure Analysis of Transmission Line Structures under Downbursts

M. Ellassaly – MEng Student, Supervisor: Dr. A.A. El Damatty
Behaviour of multi-storey braced frame timber buildings

W. Mohamed – MEng Student, Supervisor: Dr. A. A. El Damatty
Optimization of design of transmission lines under downbursts

C. Peng – MEng Student, Supervisor: Dr. A. A. El Damatty
Performance based design of buildings under wind loading

K. Dennis – PhD Candidate, Supervisor: Dr. K. Siddiqui
Characterization of three-dimensional flow structure in boundary layers over a heated flat plate

K. Teather – PhD Candidate, Supervisor: Dr. K. Siddiqui
Investigation of pore-scale phase change process in PCM-embedded porous media

E. Blokker – MEng Student, Supervisor: Dr. K. Siddiqui
Investigation of radiation heat transfer in a porous solar thermal receiver

Z. Charran – MEng Student, Supervisor: Dr. K. Siddiqui
Design and characterization of optical guide for concentrated solar energy transmission

S. Jevnikar – MEng Student, Supervisor: Dr. K. Siddiqui
Investigation of flow behavior in the transient liquid phase of a PCM thermal storage

M. Kuska – MEng Student, Supervisor: Dr. K. Siddiqui
Investigation of aquaculture pond's thermal regulation via geothermal ground loop

M. Mahaffy – MEng Student, Supervisor: Dr. K. Siddiqui
Characterization of the afterburner performance in jet engines

K. Toxopeus – MEng Student, Supervisor: Dr. K. Siddiqui
Investigation of flow behavior in a PCM-embedded flow channel

M. M. Allaf – Postdoctoral Fellow, Supervisor: Dr. H. Peerhossaini
Active fluid mechanics and biology

Z. Habibi – PhD Candidate, Supervisor: Dr. H. Peerhossaini
Mechanics of active fluids – cell-cell interactions

Z. Samadi – PhD student, Supervisor: Dr. H. Peerhossaini
Active fluids – numerical simulations

Facilities and Equipment

WindEEE Dome

The Wind Engineering, Energy and Environment (WindEEE) Dome, see Hangan (2014), is the world's first 3D wind chamber, consisting of a hexagonal test area 25m in diameter and an outer return dome 40m in diameter. Mounted on the peripheral walls and on top of the test chamber are a total of 106 individually controlled fans and 202 louver systems. Additional subsystems, including an active boundary layer floor and "guillotine" allow for further manipulation of the flow. These systems are integrated via a sophisticated control system which allows manipulation with thousands of degrees of freedom to produce various flows including straight flows, boundary layer flows, shear flows, gusts, downbursts and tornados. A pair of 5m diameter turntables as well as removable contraction systems accommodate a wide variety of test objects and wind speeds for testing inside and outside.

The WindEEE facility is certified LEEDs Silver and includes office space for industry, researchers, staff and graduate students as well as meeting and conference spaces for collaboration.

Model WindEEE Dome (MWD)

The Model WindEEE Dome (MWD) is a 1:11 scale version of the WindEEE Dome. The MWD was originally used as part of the design validation for the full-scale facility and underwent significant flow studies. The MWD has many of the same features as the full scale WindEEE Dome and can produce the same flow scenarios. The model is located on the main Western University campus at the Boundary Layer Wind Tunnel Laboratory. Because of its inexpensive operation and maintenance costs, the MWD will continue to serve as a tool for preliminary test validation/set-up, fundamental tornado research and demonstrations.



Testing Capabilities

The WindEEE Dome can accommodate multi-scale, three dimensional and time dependent wind testing that no other facility can reproduce. WindEEE can be operated in a variety of configurations:

Straight Flow Closed Loop

- Straight flow closed loop utilizing one wall of 60 fans (4 high X 15 wide)
- Up to 30m/s with removable contraction
- Test section 14m wide, 25m long and 3.8m high
- Removable slotted wall assemblies
- All types of naturally occurring horizontal flows including: uniform, gusting, sheared and boundary layer flows
- Active floor roughness control
- Wide variety of scales up to 1:1

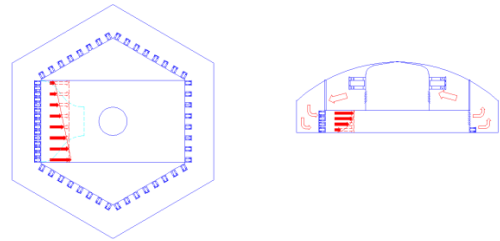


Figure 1 – Straight Flow Closed Loop

Straight Flow Open Loop

- Open mode utilizing 60 fans in reverse
- Uniform, gusting, sheared and boundary layer flows
- Up to 40m/s with removable contraction
- 5m diameter high capacity turntable
- Outdoor test platform with
- Wind driven rain, debris and destructive testing
- Access for very large full-scale test objects

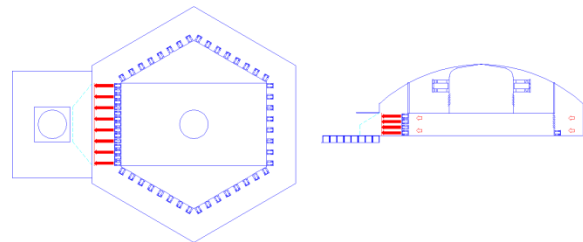


Figure 2 – Straight Flow Open Loop

Tornado

- Replication of EF0-EF3 tornados
- Properly scaled tornado flow
- Geometric scale 1/50 to 1/200
- Velocity scale 1/3 to 1/5
- Variable swirl ratio
- Adjustable vortex diameter up to 4.5m
- 2m/s maximum tornado translation speed
- Floor roughness control

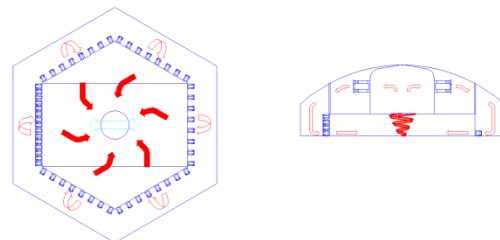


Figure 3 – Tornado

Downburst/Microburst

- Variable jet diameter (max 4.5m)
- Geometric scale $\sim 1/100$
- 2m/s maximum downburst translation speed
- Max 50m/s horizontal velocity
- Variable downburst offset and jet angle
- Combined horizontal and downward flows

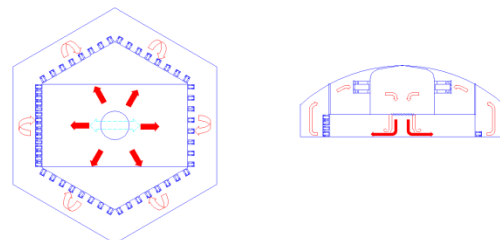


Figure 4 - Downburst

Example Uses

WindEEE Dome has been utilized for many different types of projects and we are always discovering new uses for the facility and equipment. Just like the design of the facility, many of WindEEE's capabilities are unique in the world. WindEEE allows for the first-time comparative testing of atmospheric boundary layer, downburst and tornado flows at the same scale. This allows for comparison of loads and responses of a given structure when exposed to these different wind events.



WindEEE's different flow configurations can be used to determine pressures and dynamic response of various structures. Scale models of buildings (residential, commercial, industrial, hospital, high-rise), bridges, transmission towers, wind turbines and many others can be tested. Various techniques are used to simulate the effect of surrounding buildings, topography and canopy in order to replicate the local site conditions.



WindEEE can also be used to test large scale, prototype or full-scale objects to a wide variety of wind fields. Applications range from testing of full-scale solar panels and small wind turbines, large scale

topographic and canopy models, large- and full-scale wind turbine components (blades, towers), building components, environmental measurement devices, unmanned flying vehicles, etc.



Equipment

The WindEEE Facility is furnished with a suite of equipment, instrumentation and data acquisition systems to fabricate scale models and facilitate all types of wind related research and testing, including:

- High speed/high precision pressure scanning system
- Cobra probes
- 6 DOF force balances (multiple ranges)
- Pollution/scent dispersion system
- Multi camera Particle Image Velocimetry (PIV)
- Mobile LIDAR
- Full scale monitoring systems (masts, weather station, anemometers)
- Adjustable rain rake
- 6 DOF probe traverse system
- National Instruments data acquisition systems
- CNC hotwire
- CNC router
- FDM 3D printer



References

Hangan, H., 2014. "The Wind Engineering Energy and Environment (WindEEE) Dome at Western University, Canada", Wind Engineers, JAWE, Vol. 39pp.35

Research

Wind Engineering

- Tornado wind loading on essential buildings
- Tornado induced external and internal pressures on low rise buildings
- Downburst effects on utility transmission lines
- Wind loading on full scale roof mounted solar panels
- Wind effects on ground mounted solar panels
- Destructive testing on prototype buildings
- Numerical simulations of tornadic and downburst flows
- Finite Element Analysis of collapse modes due to wind

Wind Energy

- Aerodynamic testing of smart blades
- Aeroelastic testing of model scale wind turbines
- Topography and canopy effects
- Full-scale campaigns

Wind Environment

- Wind resource assessment in complex urban environments
- Smart cities and buildings
- Wind-driven rain/snow
- Pollution-dispersion studies
- Effect of complex flows on unmanned flying object

Flow properties for a large-scale tornado-like vortex

In the field of wind engineering, the study of tornadoes is one of the most pressing research topics due to the damage of intensive tornadoes, especially in North America. The proper scaling of tornadoes is a quintessential part in modeling for any experimental or numerical study on the effects of tornadic winds on engineered structures. In this regard, laboratory simulations of tornado-like vortices have the advantage of controlled conditions and repeatability. The Wind Engineering, Energy and Environment (WindEEE) Dome at Western University already demonstrated its capacity to generate tornado-like vortices between length scales of 1/300 and 1/150 by only using the upper 6 fans and the louver system (Mode A). The research of large-scale tornado vortices in the range of 1/150 and 1/50 requires a new experimental operating mode at windEEE (Mode B). In addition to the 6 upper fans and the louvers, Mode B also utilizes the peripheral fans situated in the testing chamber. This new simulated tornado is compared and scaled against published Doppler radar data from real tornados. Analysis showed that the WindEEE Dome large-scale tornado simulations correspond to EF0 to low-end EF2-rated twisters in nature. In the field of experimental investigation in tornado actions on structures in terms of aeroelastic modeling the wind-structure interactions, these findings are particularly important.

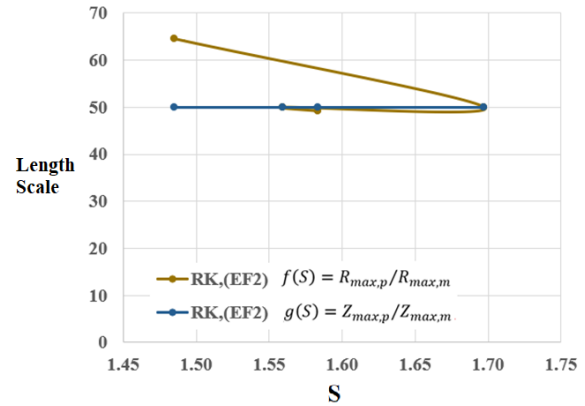


Figure 1: Geometry and velocity scale for the simulated Mode B tornado obtained using radar measurements of the real RK tornado event



Figure 2: Comparing Mode A & B by smoke test

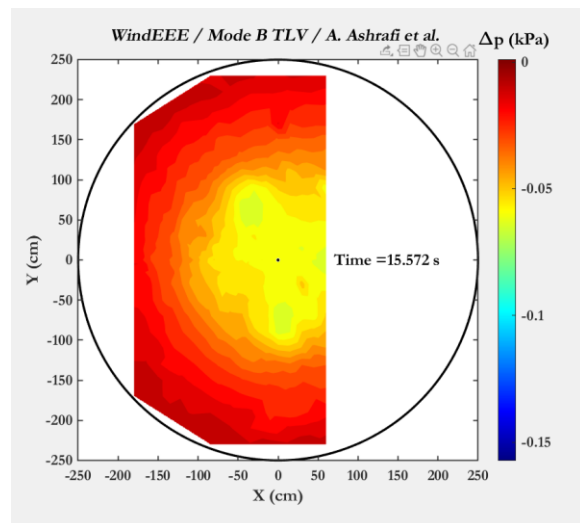


Figure 3: Pressure deficit contour on the surface of turntable

Arash Ashrafi / aashra22@uwo.ca
 Djordje Romanic / dromanica@uwo.ca
 Horia Hangan / hmhangan@uwo.ca

Combined wind and ice loading on transmission lines

During the wintertime in Canada, one of the major concerns when it comes to transmission lines are the wind and ice hazards. The wind speed in addition with the ice accretion in the conductor can produce serious damages to the towers, insulators, or even produce the entire collapse of transmission line systems. While these two hazards have been widely studied separately, there are still some uncertainties on how to deal with them as a joint hazard. For this reason, this research project focuses on the analysis of ice accretion and wind speed for a transmission line system located in the long lake site in British Columbia, specifically, the conductor of the tower 16, located at an altitude of 1490 m.a.s.l.

The project is divided into two parts:

1. Statistical analysis of wind and ice data in order to obtain static loads on the conductor.
2. Use the data obtained in the first part and perform one-way fluid structure interaction (FSI) in order to know the dynamic loads and displacements in the cable

For the first step, 19 weather stations (between 1300 and 1600 m.a.s.l.) in British Columbia were analyzed and compare with the simulated data from Kjeller Vindteknikk (2016) for the same specific site. After comparing the 50-year return period velocities, 4 out of the 19 weather stations were found to have high similarities with the simulated data. These 4 stations were used to perform a simple ice accretion model proposed by Jones (1998) which consider wind speed and hourly precipitation rate as main variables. Following the approximation used by Sinh et al. (2016), the data from the four stations were used to create just one station which contains all the data. If the icing events occurred at the same date, the most severe of the 4 were taken into consideration. Table 1 shows a comparison of the 50-year return period for wind velocity and ice accretion between historical and simulated data.

Table 1. 50-year return period comparison between historical and simulated data

Comparison	$V \left(\frac{m}{s} \right)$	Req (cm)
Simulated	43.62	10.66
Historical	59.7	8.87

The wind speed and ice accretion return periods were calculated using extreme value analysis following a Gumbel and a Peak Over Threshold (Generalized Pareto Distribution) distribution respectively. With the wind speed and ice accretion data pairs, it was possible to build the joint histogram and the joint cumulative density function in order to finally obtain joint hazard contours of probability of exceedance and mean year recurrence interval. Figure 1 shows hazard contours of 2% probability of exceedance and 50-year mean recurrence interval for historical and simulated data.

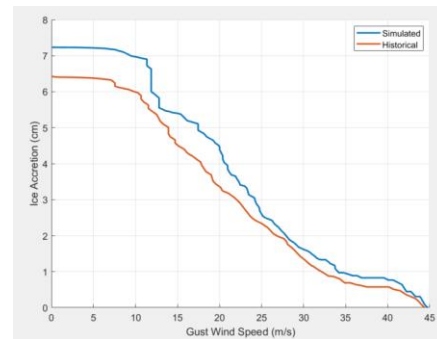


Figure 2. Hazard contours from historical (the 4 weather stations) and simulated (WRF model) data

From the historical data, the following combinations of factors for obtaining the static loads are proposed:

$$1.0 V_m + 0.2 I_m$$

$$0.4 V_m + 0.7 I_m$$

where V_m and I_m are the wind and ice loads considering the maximum velocity and ice accretion during icing conditions respectively.

The next stage of this project is to perform one-way FSI using a simple finite element model and try to obtain the dynamic loads due to wind velocity and ice accretion, as well as the displacement of the cables.

Daniel Davalos / ddavalos@uwo.ca

Horia Hangan / hmhangan@uwo.ca

Aerodynamic loading of a typical low-rise building for an experimental stationary and non-Gaussian impinging jet

To better understand the effect of stationary non-Gaussian winds on the wind loads of a typical low-rise building, a series of tests have been performed in the large test chamber at the WindEEE Dome. A continuous radial impinging jet (IJ) was used for the first time to replicate an intermediate (i.e., stationary but non-Gaussian) wind event recorded at the Port of La Spezia in Italy. The experiment was designed to quantitatively investigate the effects of these intermediate wind events on the building surface pressure distributions for three different building orientations. In addition, pressure distributions on the same building model for atmospheric boundary layer (ABL) flow (i.e., stationary and Gaussian) at the WindEEE Dome are compared with the pressure distributions from the IJ flow. Moreover, wind loads at different zones, as defined by the ASCE building code, are calculated and compared among WindEEE IJ, WindEEE ABL, NIST Aerodynamic Database and the code itself.

The intermediate wind event created by the continuous radial IJ at WindEEE is stationary with statistical non-Gaussian properties like the event recorded at the Port of La Spezia in Italy. Skewness, kurtosis, peak wind speed, gust factor and turbulence intensity between the two records (WindEEE and full scale) are compared to characterize the IJ flow at WindEEE as well as to obtain scales. Corresponding scales between WindEEE and full-scale event are; velocity 1:1.2, time 1:84 and length 1:101.

The mean pressure coefficient (C_p) distributions on the building surfaces are found to be similar between the IJ and the ABL cases, with mean roof suction higher on the roof close to the eave for ABL compared to IJ (difference in minimum mean C_p s is 16.5%). However, when 3 s peak C_p s is compared, the IJ produced localized higher roof suction than ABL especially for the corner angle case (difference in

minimum 3 s peak C_p s is 20.1%). Fluctuations of C_p s, represented by standard deviation, are higher in ABL compared to the IJ (difference in maximum standard deviation of C_p s is 14.3%). Noticeable difference in C_p fluctuations between IJ and ABL is observed in the distribution of standard deviation of C_p on the building surface where distribution is less symmetric and uniform for IJ than ABL. Apart from the non-Gaussian characteristics of IJ, the differences in velocity profiles and building height turbulence intensities between ABL and IJ could have influenced C_p s. When wind loads are compared with the ASCE standard, it is found that except for one zone on the roof (Zone F), the ASCE standard provides conservative design loads for the building orientations (0°, 57° and 90°) tested in this study.

At the end, it is important to acknowledge that this topic deserves a lot of additional research from experimental point of view. This paper presented an attempt to experimentally simulate this class of winds using IJ approach, but other options will also be explored in the future. While this study is a continuation of the previously published work in intermediate wind events, it can also serve as the starting point for experimental research of non-Gaussian, stationary wind events. At the same time, it is equally important to have more complete understanding of these winds regarding their dynamics and climatology at full scale. This gap of knowledge regarding experimental investigation of intermediate winds, on one side, and their meteorological description, on the other side, calls for an interdisciplinary research initiative between wind engineering and atmospheric sciences communities. In addition, the experiments in this study were compared against a single full-scale event. Lastly, in order to draw general conclusions regarding wind actions from intermediate winds, an ensemble averaging of multiple non-Gaussian wind events is needed.

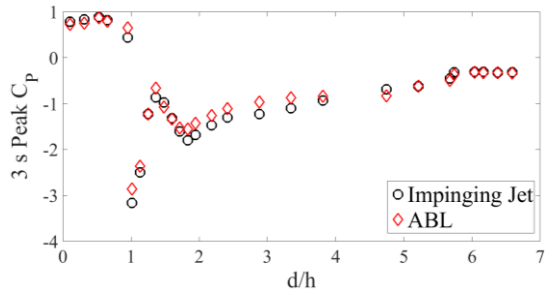


Figure 1: Comparison of the 3-s peak C_p profiles between IJ and ABL flows in the WindEEE Dome. In this case, the building was oriented so that the radial velocity component acts towards the high density tap corner on the roof of the building at 57° with the short edge of the building footprint.

Jubayer Chowdhury / cjubaye@uwo.ca

Djordje Romanic / dromanica@uwo.ca

Horia Hangan / hmhangan@uwo.ca

Flow field dynamics of large-scale experimentally produced downburst flows

This study investigated the mean and turbulent features of experimentally produced downbursts with respect to height-to-diameter (H/D) ratios and Reynolds numbers (Re). Point velocity measurements with high temporal resolution are obtained using Cobra probes for $H/D = 1.2$ and $H/D = 0.8$, as well as for a range of the values of Re (between $Re = 1.82 \times 10^6$ and $Re = 4.24 \times 10^6$). In addition, two-dimensional (2D) planar velocity measurements using large-scale particle image velocimetry (PIV) technique were conducted. Wind velocity data were decomposed into the transient mean and transient turbulence components based on the criteria set in literature. A wide range of values for the moving average times (T_{avg})—from 0.01 to 0.3 s—was investigated with respect to several criteria: (1) characteristics of running mean and residual fluctuations, (2) joint Fourier transforms of running mean and residual fluctuations, and (3) mean, standard deviation, skewness and kurtosis of reduced turbulent fluctuations. Based on this analysis, $T_{avg} = 0.1$ s was deemed to be a reasonable averaging time for the simulated downbursts in the WindEEE Dome.

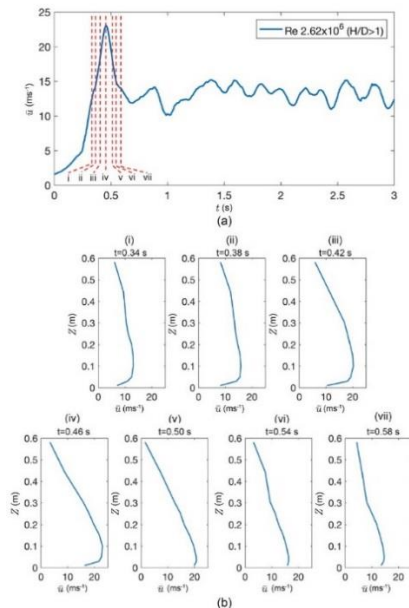


Figure 1: Time series of slowly-varying mean velocity (\bar{u}) and vertical profiles of \bar{u} at different time instances.

Profiles of time varying means of radial velocities with height are calculated for different values of Re and normalized profiles are compared against previously published full-scale data. At similar Re , the profiles corresponding to $H/D > 1$ have a more pronounced “nose” shape when compared to the ones for $H/D < 1$. Overall, the profiles corresponding to the case of $H/D > 1$, especially at lower Re (1.82×10^6 to 2.68×10^6) show better comparison with the existing full-scale data.

Finally, the vortex dynamics obtained from the PIV measurements for the experimentally simulated downbursts in the WindEEE Dome is compared with the available full-scale data. For the first time, the relative location of the primary vortex centre with respect to the maximum radial velocity, convective velocity of the primary vortex, heights and trajectory of the primary vortex centre are compared between laboratory simulated downbursts and full-scale downburst records, and promising agreement is found.

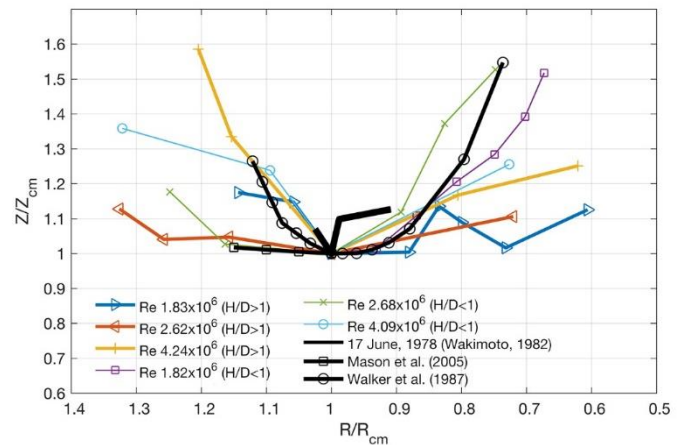


Figure 2: Normalized vortex trajectories from the WindEEE Dome downbursts compared against full-scale event on 17 June 1978.

Junayed Chowdhury / cjunayed@uwo.ca
Jubayer Chowdhury / cjubaye@uwo.ca
Dan Parvu / dparvu@uwo.ca
Djordje Romanic / dromanic@uwo.ca
Horia Hangan / hmhangan@uwo.ca

Three-dimensional measurements of tree crown movement using Kinect

The mechanical response of a tree to wind is relatively unknown and hard to quantify because of the tree's complex structure. Researchers have used marked points on the tree (Der Loughian et al. (2014)), biaxial clinometers (Bunce et al. (2019)), finite element analysis (Yang et al. (2019)), or a modified PIV (Barbacci et al. (2014)) to visualize and measure the displacement of a tree under different wind speeds. These methods are either invasive, resource consuming or lack the inclusion of the third dimension. In order to understand the wind induced motion and the variability of the tree frontal area with wind, the gap for three-dimensional physical non-invasive analysis needs to be filled.

The objective of this research is to study the behavior of a tree canopy in turbulent winds in 3D space in a fast and efficient manner. By using the sensor of a gaming console this objective has been achieved. A better overview of the movement of a tree canopy under various turbulent winds is accomplished in a novel, efficient, non-invasive and accurate way.

The tests for the study were carried out at the Wind Engineering, Energy and Environment (WindEEE) Dome in London, Ontario, Canada. A small garden tree was placed under turbulent conditions and its three-dimensional movement was captured with a gaming console sensor. The drag force and the wind velocities were measured with a force moment sensor and with pressure probes respectively.

The images captured with the gaming console sensor contain the depth precision for each pixel and therefore the position of the canopy in a three-dimensional form can be extracted at any moment in time. Also, because of the ability to access the third dimension, different new methods for determining the mean canopy area were tested and thus the correlation between the wind force exerted on the

tree crown and the resulting projected area was analyzed.

In the figures below one can see the movement of the canopy center obtained from analyzing the photos captured with the gaming console sensor.

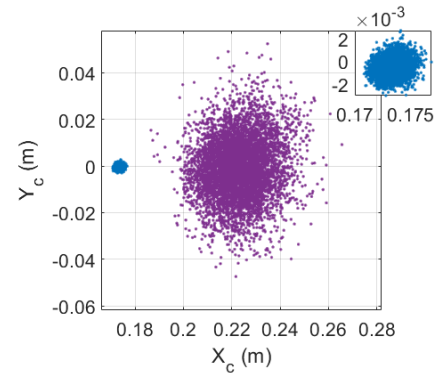


Figure 1: The movement of the tree canopy center at 1.4436m/s (blue) and 6.3378m/s (purple) wind speed on the X and Y axes.

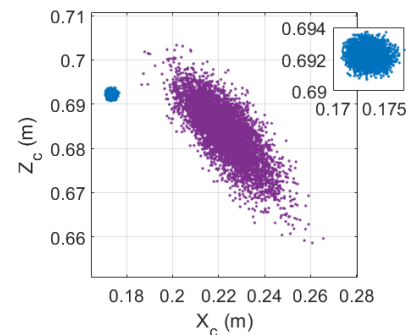


Figure 2: The movement of the tree canopy center at 1.4436m/s (blue) and 6.3378m/s (purple) wind speed on the X and Z axes.

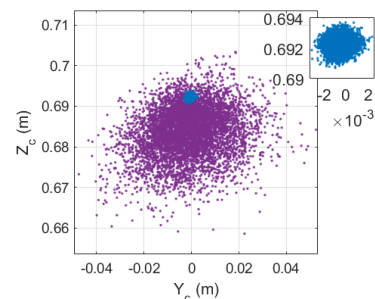


Figure 3: The movement of the tree canopy center at 1.4436m/s (blue) and 6.3378m/s (purple) wind speed on the Y and Z axes.

Marilena Enuş / menus2@uwo.ca
Horia Hangan / hmhangan@uwo.ca

Modeling of tornado-like vortices: mean and fluctuations

The evaluation of tornadic wind loads on structures highly depends on the accurate reconstruction of the tornado wind field. Besides, numerical and experimental simulations of tornado-like vortices, analytical modelling is attractive since it can be employed in risk analysis models. Major barriers to evaluate tornado wind loads exist at different levels; there is a scarcity of field data on tornado wind fields within the lower atmospheric boundary layer level creating a gap both in estimating design wind speeds and obtaining target flow characteristics for laboratory simulations and there is a lack of laboratory methods to model tornado interaction with buildings.

In this study, the velocity field of tornado-like vortices with single-cell and double-cell structures is analytically modeled. Both the mean and fluctuating flow fields are considered. The mean flow field is modeled using a combination of Burgers-Rott model and stagnation flow. Modal analysis of experimentally generated tornado-like vortices (M. Karami et. al., 2019) has shown that the large-scale fluctuating flow field can be attributed to two phenomena: (i) random displacement of the vortex (wandering motion), and (ii) sub-vortex dynamics (coherent structures). Herein, the wandering motion of the vortex is modeled by a convolution integral approach. The sub-vortex dynamics is modeled based on the reduced vorticity field resulting from the modal analysis (Proper Orthogonal Decomposition).

The extracted coherent structures identified by proper orthogonal decomposition are shown in the Figure. For $S=0.22$, a single vortex subjected to random wandering motion. For $S=0.57$, a recirculation bubble vortex at the center and a spiral vortex rotating around the bubble. For $S=0.96$, a recirculation bubble vortex at the center and a double spiral vortex rotating around the bubble.

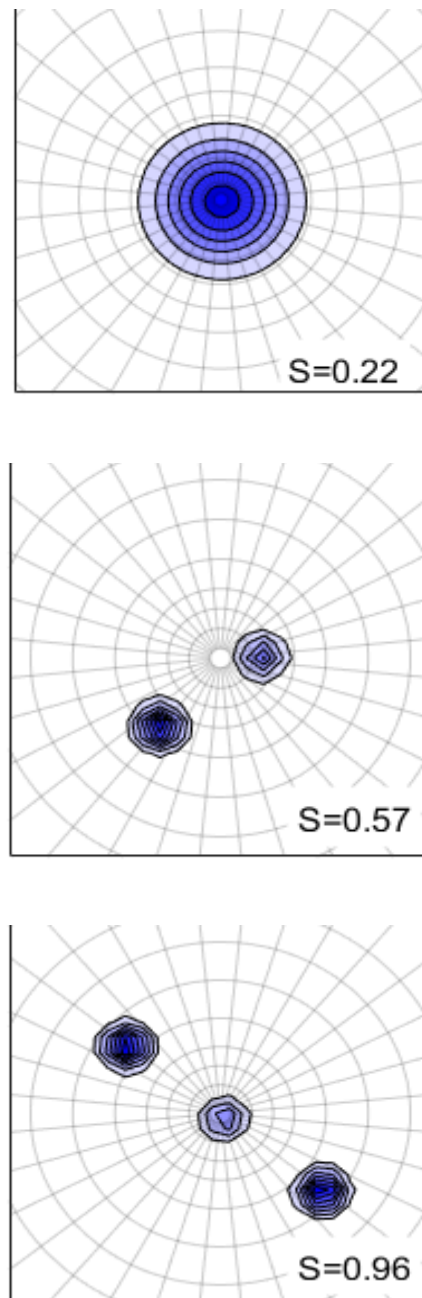


Figure 1: Schematic representation of vorticity field of coherent structures for three different swirl ratios, $S=0.22$, $S=0.57$ and $S=0.96$.

Mohammad Karami / mkarami3@uwo.ca
Horia Hangan / hmhangan@uwo.ca

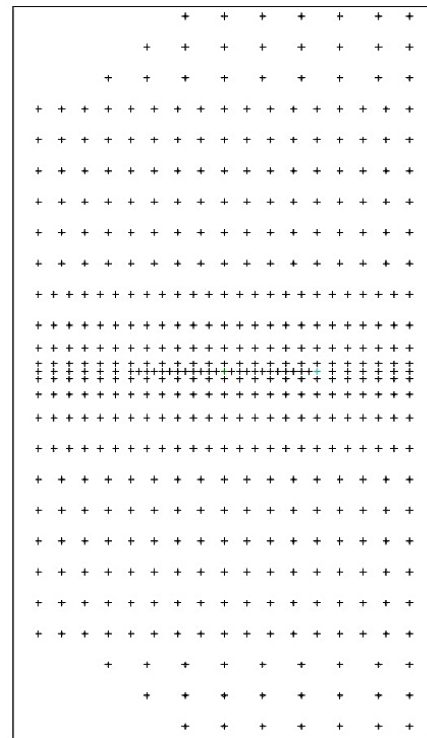
Surface pressure measurements under translating tornado-like vortices

Tornadoes are considered one of the most violent kinds of storms in history. The complexity of tornadoes arises from their 3-dimensional and turbulent nature. Nearly over 1,000 tornadoes are reported annually in the United States and their damages can exceed over one billion dollars (NOAA, 2012). Due to their danger and unpredictable behavior, few field tornado measurements have been documented.

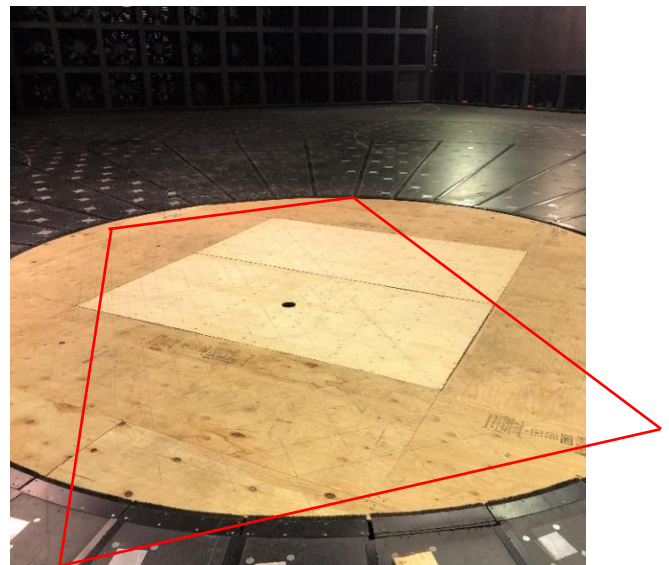
Tornado field measurements started in the mid-20th century. These difficult to obtain measurements were limited to higher heights from the ground. This is because the radars need to be fixed distant from tornado, so they had to be positioned above obstacles to get through the tornado vortex and give acceptable recordings. Another shortcoming of most of the field recordings is their low frequency. These limitations lead to the rising of experimental work using tornado vortex chambers and numerical simulations which enables near ground exploration of tornadoes.

In this study, tests were conducted at the state-of-the-art tornado simulator, the WindEEE Dome. Ground pressure measurements were carried out for a wide range of swirl ratios. Stationary and translating tornado-like vortices were tested which acquired to cover a large area with pressure taps (Fig. 1). Surface roughness was added to further examine the tornado flow field characteristics under different terrains.

Aya Kassab / akassab@uwo.ca
Jubayer Chowdhury / cjubaye@uwo.ca
Horia Hangan / hmhangan@uwo.ca



(a)



(b)

Figure 1: Base plate taps layout (a) schematic, and (b) at WindEEE

Environmental impacts of high intensity winds on communities

Although research on tornadic flows has been extensive in previous decades, the understanding of its effects on buildings and structures is limited. In particular, the pressure distribution on facades of buildings and loadings on them are poorly understood. In order to improve tornado resilience and reduce the damage associated with these events, research must be done to evaluate the loadings on real communities. On the other hand, it is important to quantify the loss that a certain tornado can create in a community. For that purpose, fragility curves must be developed.

In this project, the calculation of pressures and loadings under different extreme wind events are made for two real communities. One situated in Kansas, in the heart of “Tornado Alley” and the other in Dunrobin, Ontario. The former location was hit by an EF3 tornado in September 21, 2018. This is done through physical simulation at the WindEEE Dome, Western University. As mentioned before, the other objective of this project is to combine the loading on buildings with fragility curves to quantify the loss in property value. Finally, the results will be compared with data from real events compiled by ICLR.

Edmundo Gabriel Narancio / enaranci@uwo.ca
Horia Hangan / hmhangan@uwo.ca

Monte Carlo modelling of tornado losses on residential buildings

This research presents an updated version of the tornado loss assessment model by Romanic *et al.* (2016) (hereafter R2016). The main four modifications from R2016 are, (1) The new model is extended beyond the state of Oklahoma (OK) and now includes the state of Kansas (KS), both of which are within “Tornado Alley” in the United States (US). (2) An updated exposure map that provides the number of residential houses on a block group level is used instead of estimating the number of houses using the population density. In addition, the new model explicitly models the number of houses in each block group assuming a uniform distribution within the block group. For each tornado event, the number of affected houses is determined by calculating the overlap area of the tornado track and the affected block. (2) The new model introduces fragility curves developed for one- and two-family wood frame residences in the US as an intermediate step between tornado strength and the replacement cost. This approach accounts for the possibility of different degrees of damage that the affected house can be in under the same tornado.

The replacement cost is then based on the degree of damage instead of directly relating it to wind speed, as it was in the R2016 model. (3) The tornado vortex is analytically modelled using either the Rankine Vortex (RV) or the Modified Rankin Vortex (MRV) models. Therefore, the variability of tangential velocity across the tornado width is based on an analytical formulation, while the variability of tornado intensity across the tornado track length is adopted from literature. Other analytical formulations for the tornado vortex can easily be implemented in the current model. (4) Lastly, the new model provides easier handling of different modelling scenarios such as the isolated tornado tracks of any Enhanced Fujita (EF) scale, orientation and area, as well as their geographical placement. The model can also be easily restricted to cover only a limited geographic region.

The presented model shows that the tornado damage on one- and two-family residential houses in the KS and OK can be significant. The average aggregated loss (AGG) for the high return periods (RP) of 1000 years is US\$ 392,080,526.8 for KS and US\$ 641,281,336.0 for OK. For a small value of RP, such as 10 years, the values are US\$ 7,762,817.8 and US\$ 18,689,264.8, respectively. When compared against the R2016 model for the state of OK, these values are approximately 1.6 and 3.6 times smaller, respectively. The main reasons for the smaller loss predictions of the current model is the introduction of fragility curves and the smaller values of the empirically determined damage ratios in vulnerability relationship.

In addition, insured losses are sensitive to a variety of other conditions not modelled herein (e.g., commercial and industrial losses, business interactions, etc.). The likely occurrence of tornado outbreaks is also not considered in the current work but will be included in the future version of this model.

In terms of geographically and temporary limited simulations, we analyzed the losses inflicted by a single tornado track over a suburban area in Oklahoma City, OK. While the geometry and orientation of the track were fixed, all tornado intensities were considered (EF0–EF5). Our results show that the largest percentage increase in the loss is observed between EF1 and EF2 tornadoes (almost 100%). The losses in these simulations (limited region and single tornado) are largely deterministic due to the unchanged initial conditions in terms of tornado characteristics, exposure map and distribution parameters.

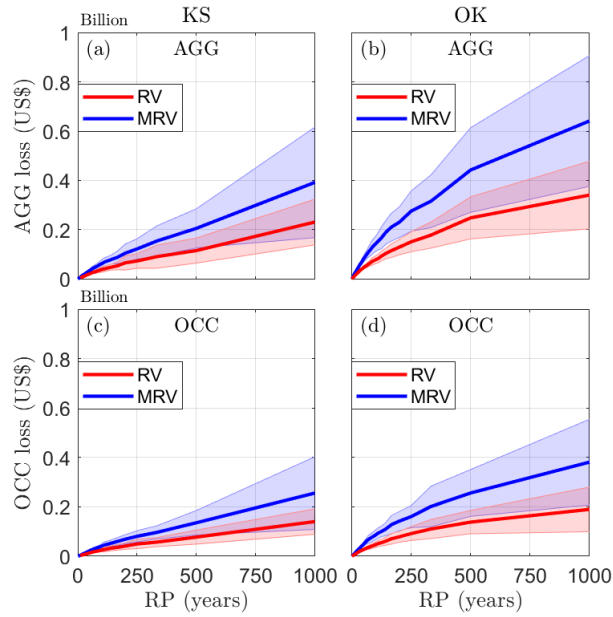


Figure 1: Exceedance probability curves showing the aggregated and occurrence losses in OK and KS using RV and MRV modules.

Maryam Refan / mrefan@uwo.ca

Djordje Romanic / dromanic@uwo.ca

Dan Parvu / dparvu@uwo.ca

Gero Michel / gerowaltermichel@gmail.com

Three-dimensional, non-stationary and non-Gaussian (3D-NS-NG) wind fields and their implications to wind-structure interaction problems

Some key aspects of the Davenport Chain related to the differences between the classical assumption that engineering structures are subjected to loads resulting from their interaction with synoptic winds and recent findings on a new class of non-synoptic winds are analyzed herein. We compare climatology, surface layer and building aerodynamics aspects related to the two type of winds and analyze the implications of their differences.

From the climatology perspective we describe downbursts and tornado type of winds in terms of their frequency, occurrence and statistics and underline the localized, three-dimensional, non-stationary and non-Gaussian characteristics of these wind compared to the assumptions of large scale, homogeneity, stationarity and Gaussianity related to the classical synoptic winds simulated based on atmospheric boundary layer (ABL) flow.

both in terms of the mean and the turbulent flow fields. We also indicate how these results can be used to drive new analytical flow models for these types of winds. We indicate ways in which both downbursts and tornadoes can be properly scaled from full scale to simulations.

From the building aerodynamics perspective, we question the assumptions related to the quasi-steady theory that is at the base of the synoptic, ABL, wind actions on structures. We show how the interaction between the building and the tornadic flow is important and how the large-scale flow fluctuations are not negligible compared to the mean flow field. We present differences between inner core and outer core tornado flow statistics in the presence of a generic building. We then use both Gaussian and non-Gaussian theory to predict pressure coefficients on a generic building and compare these predictions with direct measurements in the WindEEE Dome.

In some sense this is a review study of a work in progress. We refrained from discussing the last two links of the Davenport Chain, namely the dynamic responses and the criteria aspects, as we believe that these aspects can be better addressed by other research groups.

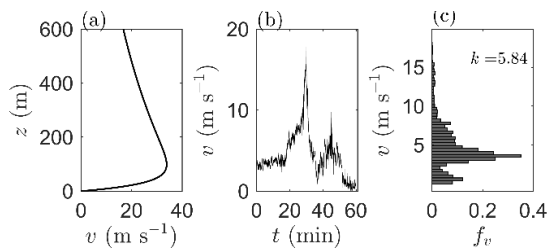


Figure 1: (a) Idealized "nose" shape profile of radial component of downburst winds. (b) Downburst velocity record measured at Livorno, Italy, on 1 October 2012 (11:35–12:35 UTC) at 20 m AGL. (c) Probability density function of the velocity record in (b) together with the value of kurtosis.

The results from the WindEEE Dome were then correlated to full scale data to provide a description of the surface layer for downbursts and tornadoes

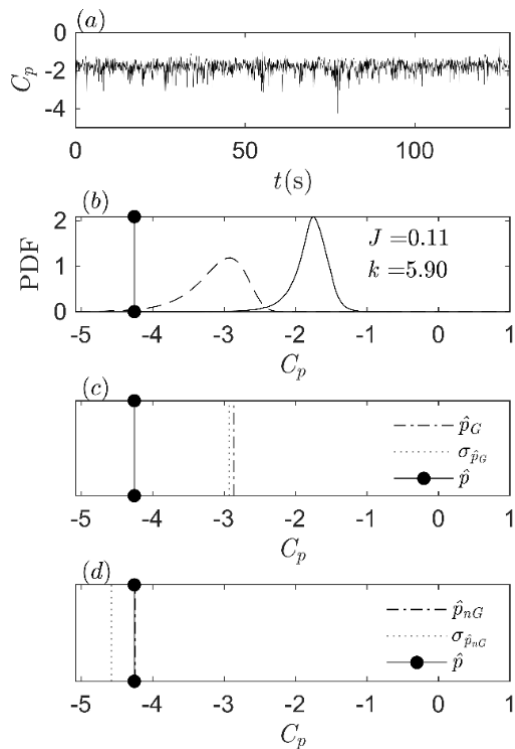


Figure 2: A time history of measured pressure coefficients (C_p s) on the surface of the building in an EF1-rated tornado in the WinDEE Dome. (b) Kernel smoothing distribution of the measured C_p s (full line) and the Gumbel distribution of C_p s (dashed line). The values of kurtosis (k) and negentropy (J) of the observed C_p s shown in (b). The actual observed minimum peak of C_p s is the vertical full line with the black symbol in all plots. (c) Predicted peak using the Gaussian method (dash-dot line) and its standard deviation (dotted line). (d) Same as (c) but using the non-Gaussian method.

Horia Hangan / hmhangan@uwo.ca
Djordje Romanic / dromanica@uwo.ca
Jubayer Chowdhury / cjubaye@uwo.ca

Transient behavior in impinging jets in crossflow with application to downburst flows

In this experiment, an impinging downburst-like jet flow (JF) was examined in the presence of the straight flow (SF) in the WindEEE Dome. Nine different strength ratios of JFs and SFs were analyzed. In addition, a novel statistical method in wind engineering and fluid dynamics for detecting the onset of a transient event was also proposed. By investigating the performance of this method for detection of abrupt changes in time series using the first and second statistical moments in terms of accuracy and computational time, a three-step algorithm was used to accurately detect the onset of simulated impinging jets in the WindEEE Dome. Moreover, this methodology successfully divided a time series of one full-scale downburst event in Livorno, Italy, into different downburst segments that are of importance when evaluating downburst wind actions on structures.

More insight into the behavior of the combined JF and SF mode in the WindEEE Dome was obtained through statistical moments and velocity profiles in the along SF and across SF directions. The negative skewness and positive kurtosis in the core of JFs are interpreted as a flow which has a large occurrence of high magnitudes of velocity and little deviation from the mean value. Velocity distribution of peripheral probes in the outskirts of jets are more Gaussian due to the larger turbulent fluctuations. Inspection of the mean velocity profiles depicted the interactions between JF and SF in both along SF and cross SF directions. The spectra of the measured flow near the edges of the jet have more energy in the higher frequency compared to those near the center, indicating more shear in the flow.

The combined JF and SF mode of operation of the WindEEE Dome can essentially be broken down into two scenarios: when the JFs are dominant over the SFs and vice versa. If the JF is stronger than the SFs no significant influence on the structure of the impinging

JF can be seen. However, noticeable changes to the shape the impinging jet are observed when the SFs overpower the JF. Increased shearing in the along SF direction and increased number of zeros in velocity time series (i.e., bad data) indicate that the outflow of the bell mouth might be more of an elliptical shape skewed in the across SF direction.

From this experiment, it can be concluded that the addition of background wind via the 60-fan wall is not detrimental to the impinging jet outflow should the JF be the dominant flow feature. When it comes to the strength of JFs, the weakest investigated jet diminishes significantly in the presence of the SFs.

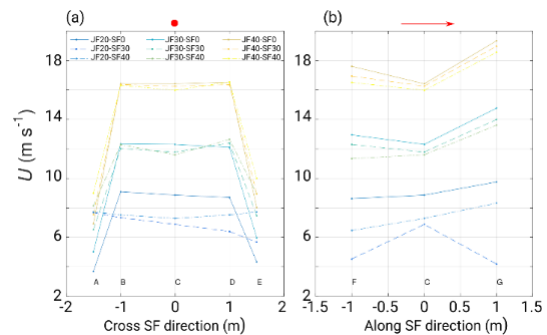


Figure 1: Velocity profiles at the bell mouth for nine different configurations of SFs and JFs tested in this study.

Several conclusions are drawn from the investigation of the relationship between the strength of SF and JF when both flows are combined. Firstly, the strongest influence of SF winds on the strength of JF is for weak impinging jets. Increasing the strength of the impinging jet drastically diminishes the differences between no-SF and SF cases. Secondly, the differences between the cases are not uniformly distributed throughout the impinging jet. The largest differences are observed for the two peripheral Cobra Probes in the cross-SF direction (probes A and E), while the smallest discrepancies between different runs are typically observed for the central probe (probe C).

Thirdly, the deviations between the mean velocities of SF winds are very small under different strengths of impinging jets if the whole time series is considered. However, if the SF velocity record is

divided into the parts before and after the impinging jet, then a noticeable slowdown of SF winds is observed. Lastly, the velocity spectra of SF winds before and after the impinging jet show some departures from the $-5/3$ slope which deserves further investigation.

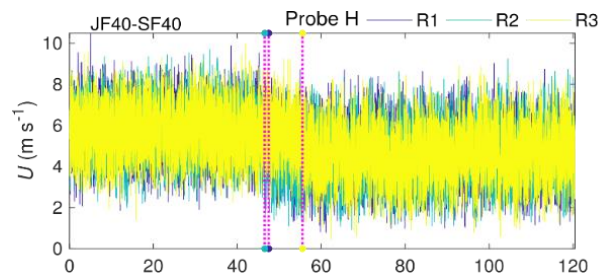


Figure 2: Decline of SF after the release of JF.

Djordje Romanic / dromanic@uwo.ca

Julien LoTufo / jlotufo@uwo.ca

Horia Hangan / hmhangan@uwo.ca

A novel approach to scaling experimentally produced downburst-like impinging jet outflows

This study introduced a novel scaling technique of downburst outflows aiming to reproduce specific downbursts detected at the full-scale, or families of these, in an experimental facility. Scaling of downburst events is a key aspect of wind engineering, both regarding laboratory simulation of the flow as well as to the investigation of downburst wind loading, wind-induced response and aeroelastic effects on structures.

The proposed method compares the γ functions of modelled downbursts in a wind simulator (m downbursts) and full-scale downburst events (p downbursts). The γ function, defined as a ratio $\bar{v}_s/\bar{v}_{\max,s}$ (where \bar{v}_s is the slowly-varying mean, $\bar{v}_{\max,s}$ is the maximum value of \bar{v}_s , and s is either p or m), describes in non-dimensional form the transient downburst time series characterized by velocity ramp-up, peak, and slowdown of wind speed. The best match between γ_p and γ_m is obtained through a parametric procedure which finds the best averaging window of m data. The scaling method was tested on 1400 m downburst records experimentally simulated in the WindEEE Dome, and on 17 p records from the Mediterranean in Italy.

First, the simulated downbursts in the WindEEE Dome closely resemble the transient features of p downbursts both qualitatively and quantitatively. This similarity is demonstrated by comparing the γ functions of p and m records and by inspecting their slope and symmetry for different averaging times. In addition, the μ functions [$\mu_s(t_s) = I_{v,s}(t_s)/\bar{I}_{v,s}$; where $I_{v,s}(t_s)$ is the slowly-varying turbulence intensity in time, t_s , and $\bar{I}_{v,s}$ is its mean value] between p and m records are also analyzed and their similarity is confirmed. While γ describe the mean feature of the flow, the μ functions describe the

fluctuating (turbulent) properties of downburst outflows. It was concluded that each γ function can be represented as a sample of a highly transient random process, whereas the μ functions are quasi-stationary and deterministic.

Second, the typical velocity and time scales between the investigated p and m records are found to be between 2:1 to 4:1 and 40:1 to 70:1, respectively. However, significant deviations from these values are also observed. The resulting length scales are obtained as the product of velocity and time scales and they are in typically around 100:1 to 250:1, and similar.

Third, the proposed scaling method is validated on several p downburst events, but only two are shown in this study—one from Genoa, Italy, that occurred on 30 September 2012 and the other from Livorno, Italy, that took place on 1 October 2012. The Genoa event was recorded with one anemometer, while the Livorno event was captured by three anemometers. The proposed scaling method accurately predicted the height of the anemometers to be around 13 m above ground level (AGL) in Genoa and at around 25 and 74 m AGL in Livorno. In addition, the scaling method enabled a partial reconstruction of the selected p events in terms of evaluating the radial distance of downburst touchdown and the radius of the maximum wind speed in the downburst outflow in respect to the anemometer positions. In all investigated cases, the downbursts were spawned above the sea and advanced toward the coast.

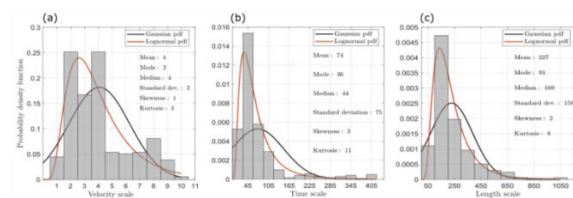


Figure 1: (a) Velocity, (b) time and (c) length scales of the WindEEE Dome downbursts.

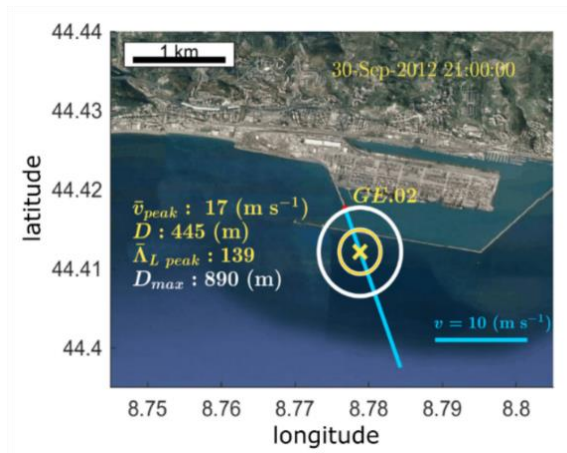


Figure 2: Partially reconstructed downburst event in Genoa, Italy, using WindEEE Dome measurements.

Djordje Romanic / dromanic@uwo.ca

Edoardo Nicolini / edoardonicolini1993@gmail.com

Horia Hangan / hmhangan@uwo.ca

Massimiliano Burlando /

massimiliano.burlando@unige.it

Giovanni Solari / giovanni.solari@unige.it

Investigation of abrupt changes (change-points) in a thunderstorm velocity record

Thunderstorm winds are characterized with high velocities and transient signature in the velocity records. The transient character of thunderstorm winds is pronounced in terms of both moving mean wind speed and turbulent fluctuations. This transient signature of thunderstorm winds is an important factor that needs to be considered when estimating thunderstorm wind actions on buildings and other objects.

This study introduces a mathematical technique that objectively segments a thunderstorm velocity time series into different parts. Each of the segments is characterized with significantly different statistical property (e.g., mean, standard deviation) than the two adjacent segments. The application of the method is presented on the case of a thunderstorm wind record from the coast of Genoa, Italy. The analyzed event is a thunderstorm velocity record from Genoa, Italy, that was recorded on 30 September 2012. The bi-axial ultrasonic anemometer that measured this event was located at the port of Genoa at 13.3 m above ground level. The anemometer sampling frequency was 10 Hz.

A 1-s velocity peak of 21 m s^{-1} was observed around 21:00 UTC. As typical for thunderstorm winds, this 1-h long time series is characterized with three main segments: (1) the thunderstorm wind segment between approximately 20:55 UTC and 21:13 UTC, (2) the background winds prior to thunderstorm (before 20:55 UTC), and (3) background winds after the thunderstorm (after 21:13 UTC). The background winds prior to and after the thunderstorm wind are below 5 m s^{-1} . The thunderstorm segment is characterized with a very rapid ramp-up which started at around 20:55 UTC and the main peak with the duration of approximately 9–10 min. The second thunderstorm peak is also about 10 min long and it started around 21:04 UTC. The velocities in the

second peak are around three to four times smaller than the velocities in the first thunderstorm peak. A change-point is the point in time series at which a certain statistical property of a segment of data change beyond a given threshold. The statistical properties that are mean and standard deviation.

The instantaneous velocity (top panel) is decomposed into the slowly-varying mean and the turbulence-related quantities. The instantaneous and slowly-varying mean time series are characterized with four segments. The first and the last segment correspond to the background ABL (steady) winds before and after the thunderstorm, respectively. In this case, the breakpoints in the standard deviation and mean coincide with each other. These findings demonstrate that the transiency of the mean flow and fluctuations occurred at the same time. Further, we observe that the residual turbulence fluctuations, the slowly-varying standard deviation and the slowly-varying turbulence intensity only have change-points in standard deviation. In terms of residual fluctuations and slowly-varying standard deviation, the second thunderstorm wind peak has the same properties as the background ABL winds. Turbulence intensity after the thunderstorm event was higher than during the event and prior to it. Lastly, the reduced turbulent fluctuations, which are stationary and Gaussian process, do not have any change-point in terms of both mean and standard deviation.

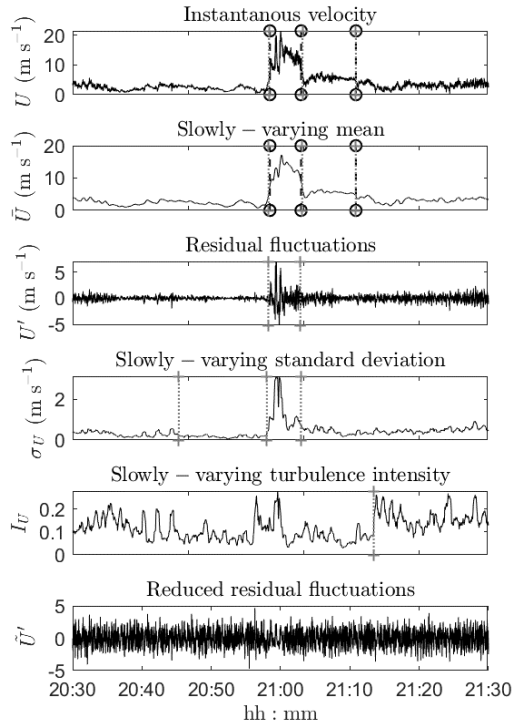


Figure 1: Decomposed thunderstorm velocity time series and location of change points. The vertical (black) dashed lines with the circular markers are the locations of change points in mean and the vertical (grey) dotted lines with the star markers are the locations of change points in the standard deviation.

Djordje Romanic / dromanic@uwo.ca
Junayed Chowdhury / cjunayed@uwo.ca
Jubayer Chowdhury / cjubaye@uwo.ca
Horia Hangan / hmhangan@uwo.ca

Dynamic structural analysis of scaled lighting pole model in physically simulated tornadic flow

The destructive power of tornadoes is so pronounced that the tornadic events are classified based on their potential to cause damages on various objects and trees. This categorization of tornadoes is known as the Enhanced Fujita (EF) scale; where EF0 and EF5 are the weakest and the strongest categories of tornadoes, respectively. Among different damage indicators (28 in total), McDonald *et al.* (2006) used damages inflicted on free-standing light poles, luminary poles and flag poles to estimate tornadoes' EF scale.

A cantilevered lighting metal pole has three Degrees of Damage (DOD). The damage indicator of DOD1 is a threshold of visible damage on the pole and the expected tornadic wind speed associated with DOD1 is 36.2 m/s. The damage indicators for DOD2 and DOD3 are bent pole and collapsed pole, respectively, with the expected wind speeds of 45.6 m/s and 52.8 m/s, respectively. The lighting poles have the simplest and the smallest number of DODs (only 3) among all other damage indicators. For example, one- or two-family residences have ten DODs which are not independent of each other and often result in a progressive collapse of the structure. Therefore, due to the simplicity of lighting pole geometry, only three DODs, and the uniformity of construction material (effectively, the whole structure is metal), a lighting pole is selected for an experimental investigation of tornadic wind actions and dynamic structural analysis.

The goals of this study carried out in WindEEE Dome are: (1) to provide the first experimental results of dynamic structural behavior of lighting poles in tornadic flow (2) to compare these results with field observations; and (3) to relate the tornadic results to the wind actions due to the straight, atmospheric boundary layer winds.

The experiment setup of 1:50 geometrically scaled light pole model was performed in the WindEEE Dome. The surface pressure measurements were obtained using two circular cylinders with the diameters of 4.0 mm and 12.5 mm. The thicker diameter represents the lower section of the generic lighting pole, while the thinner section is used to simulate the upper section of the pole. Each cylinder has 12 pressure tubes connected to pressure scanners which are used to measure differential pressure. The measurements are conducted at 8 heights: 5, 10, 23, 30, 40, 50, 60, and 73 cm above floor. The lowest two heights were represented using the thick cylinder. The model is tested for stationary and translating tornadoes and each test is repeated 5 times to ensure statistical significance of results and estimate the result uncertainties. Moreover, 3 radial positions (r/r_{max} , where r_{max} is the radius of the maximum tangential velocity, $v_{tan,max}$, i.e., the core radius) of the model in respect to tornado center were investigated: (1) $r/r_{max} = 0$; (2) $r/r_{max} = 1$; and (3) $r/r_{max} = 0.64$. In total, more than 140 tests were performed in the WindEEE Dome.

The circumferential integration of differential pressures and calculation of drag and lift pressure coefficients, C_p , are shown in the following figure. The obtained C_p s together with the scaling parameters are used to determine full scale time histories of drag (D) and lift (L) forces at each height and for each tested scenario. The force records show the pronounced transient signature. In addition, the fluctuations of D and L decrease with increasing the height above the ground.

Dynamic and non-linear structural analysis will be performed in order to obtain displacement, acceleration, and bending moments of the structure. This study will also estimate the deformation and collapse criteria of the pole and compare those findings against the full-scale observations. Moreover, an aeroelastic model of the pole will be subjected to the same tornadic flow in order to estimate non-linear wind-structure interactions. Lastly, the future work will include testing of the

lighting pole models on thunderstorm downburst winds

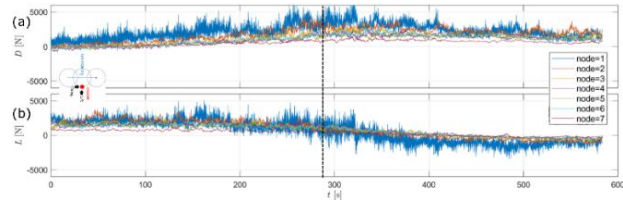


Figure 1: Drag (D) and lift (L) forces on tested lighting pole scaled up to prototype magnitudes. The vertical dashed line indicates the time when tornado center a core radius distance from the pole ($r/r_{max} = 1$).

Djordje Romanic / dromanica@uwo.ca

Hiroaki Shoji / hshoji2@uwo.ca

Horia Hangan / hmhangan@uwo.ca

Experimental investigation of tornado resilience for a modern community situated in Kansas, United States.

Horia Hangan / hmhangan@uwo.ca
Djordje Romanic / dromanica@uwo.ca
Juan Pablo Lopez / jlopezor@uwo.ca

Tornadoes are vigorously rotating columns of air capable of inflicting substantial damages on structures, as well as the entire urban or rural communities. This destructive nature of tornadoes has also been used as their classification measure through Fujita (F) scale and later Enhanced Fujita (EF) scale. While severe storms including tornadoes have the lower average event cost than tropical cyclones, droughts and inland flooding events, they are characterized with the highest number of billion-dollar damage events in the period 1980–2019 (NCEI, 2019). Therefore, their frequency of occurrence is much higher than the occurrence of other meteorological perils. Moreover, in some years the aggregated tornado losses can top the losses caused by hurricanes and other wind perils in that year (Romanic et al, 2016).

The current study presents a physical simulation of surface pressures and aerodynamic forces exerted by three different tornado-like vortices (EF1- to EF3-rated) on buildings with realistic design and in a community that is planned to be built in the state of Kansas (KS), US.

A series of tests will be realized in the Wind Engineering, Energy and Environment (WindEEE) Dome facilities at Western University. These tests will consist on examining seven different configurations of 4 low-rise buildings set influenced by 3 distinct stationary tornadic-flows (EF1- to EF3-rated), one translational EF3 tornadic-flow, and one ABL flow. The configuration variations will involve in the modification of one property in one determined building. These variations will be the orientation of the buildings relating to the vortex-core center, the displacement between two buildings and consequently to the vortex-core center, and the roof heights.

Simulating operational extreme condition for horizontal axis wind turbines based on IEC standard

The possibility of simulating some of the deterministic extreme operational conditions for horizontal axis wind turbines based on IEC 61400-1 at WindEEE Dome was investigated. For this study, using the capability of 60 fans on one wall, simulation of Extreme Operational Gust (EOG), Extreme Vertical Shear (EVS) positive and negative as well as Extreme Horizontal Shear (EHS) are considered (tailored for a 2.2 m HAWT, representing a full scale, 1:42). All these cases are deterministic and transient. The fan power set-points can be set dynamically and individually. In addition, the fans are equipped with adjustable Inlet Guiding Vanes (IGV) which can dynamically be regulated for creating different wind patterns and gusts. The study design is first to develop a numerical model for the test chamber, then approximating the fan set-ups for each different extreme condition and then comparing the flow field time history with the prescribed conditions from the standard. The final step is to investigate the effect of these conditions on power performance and loading of the model wind turbine.

At the end, the generated scenarios according to CFD predictions are in 30% range of relative error to what the standard prescribed.

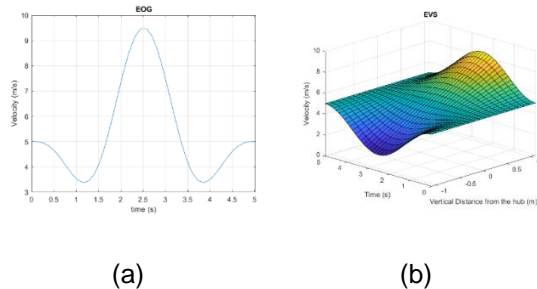


Figure 1: The desired extreme conditions for simulations and experiments based on the micro wind turbine and capability of the fans, identical to prescribed extreme condition for the full scale, (a) extreme operating gust, (b) extreme vertical shear

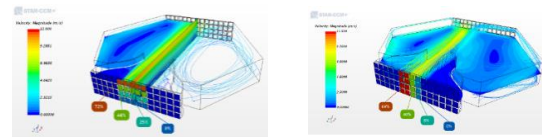


Figure 2: Simulating the fan set-ups for peak stages of extreme shears (a) vertical and (b) horizontal, prescribed for the micro HAWT identical to full scale condition.

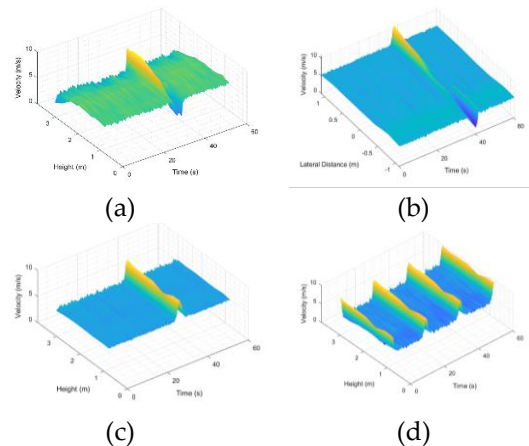


Figure 3: 3D pictures of the time history of the filtered turbulent velocity field, (a) EVS, (b) EHS, (c) EOG generated with changing fan powers, (d) EOG generated with IGVs

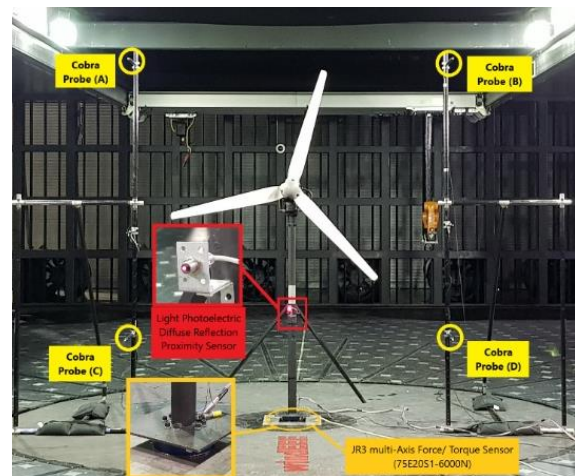


Figure 4: Set-up for measuring the effect of the transient extreme conditions on power performance and loads at the base of the tower

Kamran Shirzadeh Ajirlo / kshirzad@uwo.ca
Horia Hangan / hmhangan@uwo.ca
Curran Crawford / curranc@uvic.ca

Drone enabled automated urban topology and airflow modeling

A 3D building model is a valuable tool for researchers and city planners to make decisions. The inputs for 3D modelling are LiDAR, airborne and satellite images. One of the major challenges in realistic and pragmatic numerical urban micro-climate modeling for wind engineering, environmental and building energy simulation applications is the complexity of the geometry (topology) and the variability of surface types involved in urban exposures. Each building form and surface classification is individually and manually entered a CAD model through on-site-observations and publicly available information, which are often very time consuming and less precise. Accurate site and building specific information are required to assess climate loads such as wind, for example, during structural or environmental design. This necessitates urban climate modeling (wind speed, pressure, humidity, temperature, etc.) at high temporal and spatial resolution. The main objective of this research is developing an automated site-specific 3D urban topology and micro-climate modeling using a machine learning approach. For this purpose, various remote sensors installed on Unmanned Aerial Vehicle (UAV) will be used to collect topology and surface data. The proposed UAV based system will integrate the data collected by the Global Navigation Satellite System (GNSS), Inertial Measurement Unit (IMU), Laser, and Multi-Spectral camera to produce information on geometrical and surface properties of buildings and the ground in the neighborhoods. Digital image data acquired will be integrated with 3D cloud points collected by mobile LIDAR sensors for better data fusion and automated feature extraction to better define the geometric boundary conditions. A preliminary study for London ON downtown. The workflow starting from Airborne Lidar data, various filtered scenes, mesh used in the CFD, and sample urban wind flow field are shown in the figures.

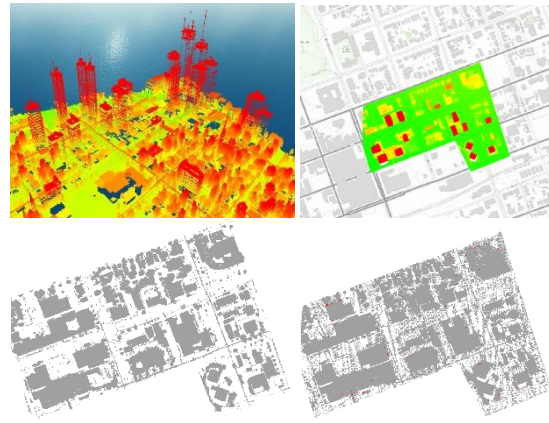


Figure 1: Airborne LiDAR 3D view of downtown area London, Ontario and various feature extraction filtering.

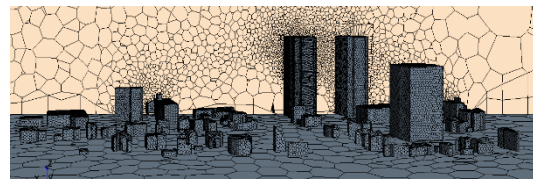


Figure 2: CFD Model Mesh Generation

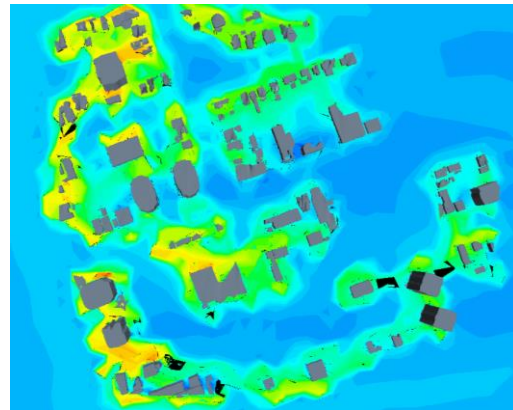


Figure 3: Wind field contour

Tewodros Alemayehu / talemaye@uwo.ca
Ahmed Shaker / ahmed.shaker@ryerson.ca
Girma Bitsuamlak / gbitsuam@uwo.ca

A Numerical study on the external convective heat transfer coefficient for buildings in different urban land-use designation

Convective heat transfer coefficient (CHTC) is an important aspect of heat exchange between a building and its surroundings. There are several correlations suggested for estimation of CHTC. However, there is a marked difference between values obtained from these correlations under similar set of conditions. Therefore, there is a need for an extensive study addressing the discrepancies in some of the existing correlations.

In the current study, the impact of built morphology, associated with different land use classes (e.g. industrial, residential, or downtown, etc.), on the convective heat transfer from buildings is numerically investigated. CFD simulations are conducted in a Navier-Stokes solver with Reynolds stress turbulence model as a closure method. The surrounding buildings are expected to influence the local microclimate (wind speed and turbulence) which in turn will affect the CHTC of the study building. Arrays of buildings from different land use class with several packing density representing different flow regimes and a benchmarking isolated cube case have been investigated. Frontal/planar densities of sections of various parts of cities, based on their land use class - from literature, are used to relate CHTC findings from simulation to land-use designation of the sites.

The results indicate that the behavior of convective heat transfer from building surfaces significantly depends on the land-use classification of the location of the study building. The results show, for each mean wind speed, that CHTC needs to be viewed as a three-dimensional response surface as a function of planar and frontal densities. For all surfaces, the highest CHTC value is obtained at a combination of high frontal and low planar density, corresponding to slender buildings with large separation spacing between them (practically rear case). This is true

because the mean ABL flow reaching the buildings is hardly affected (reduced) and the buildings' tops extend into the high mean velocity range, comparatively. The lowest CHTC zone is near to very high density in both frontal and planar, corresponding to city downtown class. This can be explained by the nearly restricted state of air flow in such density combinations. The CHTC from lateral and top surfaces peaks again in the mid-frontal and high planar density range, corresponding to low rise large span (industrial class) buildings. This is due increased turbulence near due to surrounding buildings. Mid-frontal and mid-planar density combinations corresponded roughly to the class of residential buildings.

The development of land use class based CHTC correlations are expected to reduce the bias resulting from using correlation based on isolated building studies.

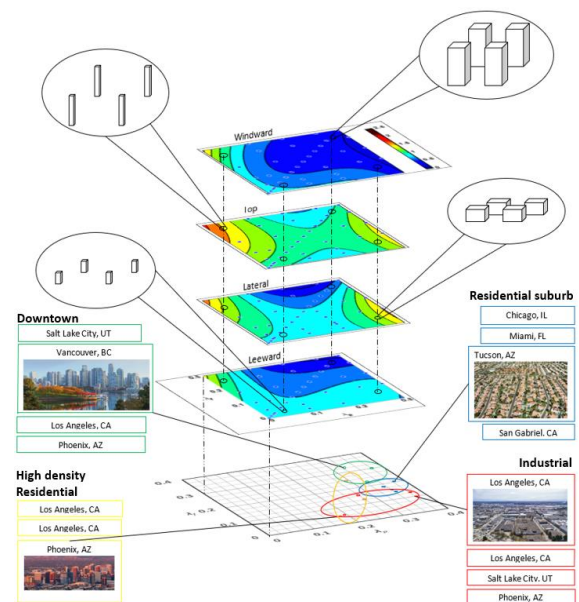


Figure 1: Contour plots of CHTC for each orientation, schematic representation of densities at the extremes, and where the physical urban densities fall

Anwar Awol / ademsis@uwo.ca

Girma Bitsuamlak / gbitsuam@uwo.ca

Fitsum Tariku / fitsum_tariku@bcit.ca

Hindcasting the damage of Ottawa-Gatineau tornado outbreak of September 2018: A computational approach

The Ottawa-Gatineau tornado outbreak of September 2018 caused 23 injuries, damaged over 2000 houses and electrical infrastructure causing a power outage that affected over 200,000 people for days following the storm. Dunrobin was identified as one of the worst hit neighborhoods in the aftermath of the event. In the aftermath of the outbreak, as the affected communities struggle to rebuild, decision makers wonder what could be done to reduce the impact of such catastrophic events. Mitigation strategies and loss estimations can be improved by better understanding of the relationship between spatio-temporally varying tornado wind field and associated structural damage. This raises the following questions: can we re-construct the tornado wind-field based on the observed damage? Can the aerodynamic and structural details of the affected houses explain the different levels and types of damage they experienced? To shed some light on these questions, a study is currently being carried out with the following objectives (i) replicating the Dunrobin tornado wind field using computational fluid dynamics (CFD) to approximately model the exposure and associated aerodynamic interaction of the buildings in the neighborhood with the tornado, (ii) conducting finite element analyses (FEA) of certain representative buildings with the tornado wind loads obtained from the CFD simulations.

In the first part of the study, preliminary CFD simulations were conducted to match the Dunrobin tornado wind field. The current state-of-the-art in tornado scaling requires the knowledge of the radial (r_{cmax}) and axial (z_{cmax}) location of the overall maximum tangential velocity (v_{tmax}), along with its magnitude, typically obtained by Doppler radar. However, due to unavailability of Doppler measurements for this event, qualitative assessment of the damage (path, width, EF rating) and available

video footages were used to make a crude estimation of the Dunrobin tornado characteristics. Further, the numerical set-up used for the current simulations requires an input tangential (v_{ti}) and radial (v_{ri}) velocity at a prescribed radius (r_0) and along a prescribed height (h_0). Thus, v_{ti} , v_{ri} , r_0 and h_0 (boundary conditions) together control the tornado characteristics (r_{cmax} , z_{cmax} and v_{tmax}). To match the output tornado characteristics with a target, it is desirable to know the output parameters for a given set of boundary conditions a-priori. Therefore, to establish a relationship between the input and output parameters in the present numerical set-up a parametric study was conducted to generate a tornado wind-field database. Simulations for a range of aspect ratios (0.25, 0.4 and 0.5) and swirl ratios (0.1-1) were conducted by changing the boundary conditions and the resulting tornado characteristics were noted.

Then a stationary vortex was calibrated to match the estimated wind field (target size and velocity) using the results from the previously conducted parametric study. A grid independence analysis was conducted for the stationary vortex. A careful grid design was particularly important since the present simulations are conducted at a full-scale and therefore at a high Re. Finally, translating tornado simulations were conducted to obtain the wind loads on the buildings in the Dunrobin neighborhood. These wind loads will now be used to conduct a finite element analysis for various structures.

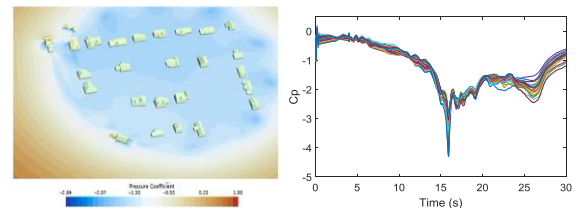


Figure 1: a) Instantaneous pressure coefficient (C_p) contour b) C_p time history sample

Anant Gairola / agairola@uwo.ca

Girma Bitsuamlak / gbitsuam@uwo.ca

LES of TTU building and its comparison to BLWT test results

Accurate evaluation of wind load using LES requires a thorough definition of boundary conditions, generation of quality mesh, selection of solvers, and proper computational domain size. Inflow generation is one of the common challenging aspects of LES for wind load evaluation. In this study, two types of inflow are used: 1) full replica of BLWT for its accuracy and robustness, and 2) synthetic CDRFG method for its versatility and ease of application. Figure 1 shows the CFD model of the BLWT used to generate inflow.

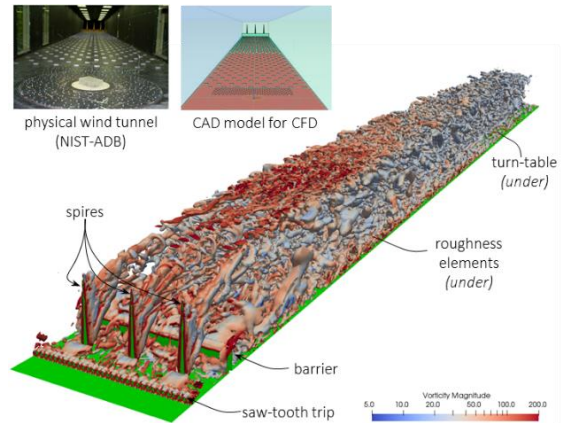


Figure 1: CFD model of BLWT to generate realistic inflow data

The wind field and terrain modeling targeted to match the BLWT test of TTU building. Figure 2 shows the instantaneous velocity field and building surface pressure coefficient C_p . Figure 3 shows the wind field characteristics and external pressure results obtained.

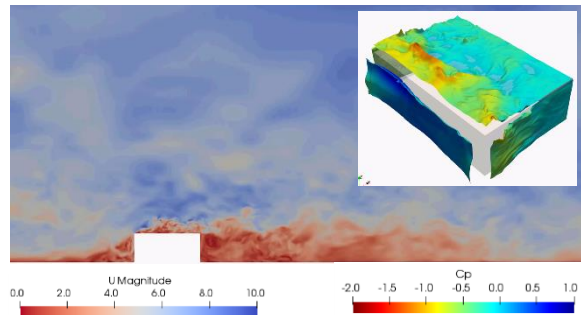


Figure 2: Instantaneous velocity magnitude along building center line and instantaneous C_p on building surface

The results obtained mostly envelope the target values. Once the wind field simulation has been validated, the building surface pressure has been compared to the target values. The comparison of mean, standard deviation and peak of external pressure coefficient C_{pE} also show a good match. For most of the cases the current results envelop the target values.

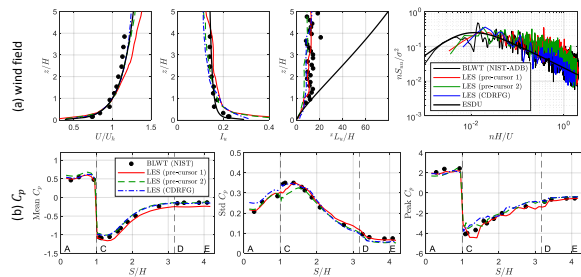


Figure 3: Validation of (a) wind field and (b) external pressure coefficient C_p

The results obtained so far indicate a promising result to proceed towards full-scale simulation. Upon achieving that, the method can potentially address some of the commonly observed scale mismatching while studying wide spectrum of test object size in wind tunnels.

Tsinuel Geleta / tgeleta@uwo.ca
Girma Bitsuamlak / gbitsuam@uwo.ca

Window configuration optimization in buildings

The need for energy efficient buildings has increased due to the increase in urban development, environmental concerns, and rising energy costs. Building façade plays a crucial role in meeting the building efficiency and internal thermal comfort demands. The primary energy use in building for heating and cooling is due to the heat flow through the façades. Window systems alone could easily be the largest heat flow contributors for buildings. Therefore, the design and selection of a proper window system is one of the most critical passive strategies for saving energy in buildings. However, when optimizing a window configuration, the heating, cooling, and lighting performance conflicts. Smaller window performs better for controlling heat loss in winter and solar heat gain in summer; while a larger window is required for better views, daylighting, and solar heat gains in winter.

Therefore, this study provides a novel framework for simulation-based optimization of window configuration on high-rise buildings. The technique involves Computational Fluid Dynamics (CFD), Building Energy Simulation (BES), and a numerical optimizer for iterative optimal window configuration selection. The objective is to minimize the annual energy consumption in a building due to heating, cooling, and electric lighting. The decision parameters are window size and room location. The thermal comfort temperature set points and daylight illuminance are taken as constraints. The proposed approach is implemented in an isolated 100 m high-rise building case study located in Boston, MA. Therefore, for a room located on the 2nd, 15th, and 29th floors an optimum window configuration of 30%, 48%, and 30%, window-to-wall ratio, respectively are obtained. Overall, architectural details, window configuration parameters, and room location have a critical impact on the betterment of the building energy performance. Therefore, choosing an appropriate window configuration based on the convective heat transfer distribution on the

façade can improve building energy performance significantly.

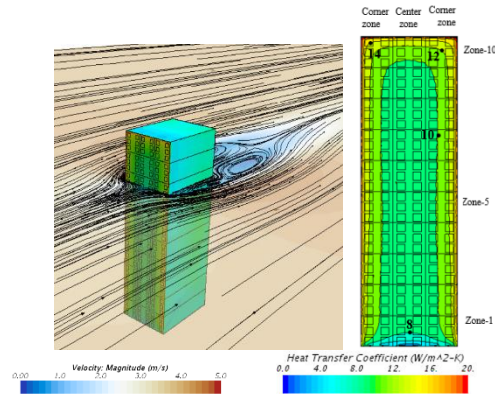


Figure 1: Velocity magnitude contours and CHTC distribution for a wind speed of 3 m/s at 10 m ref height at the inlet.

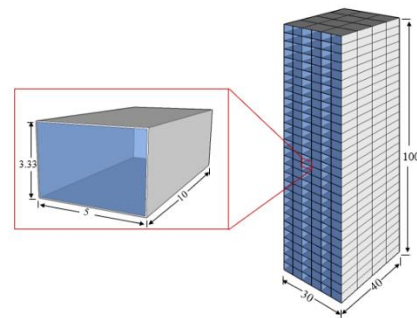


Figure 2: Schematic view of energy analysis baseline model

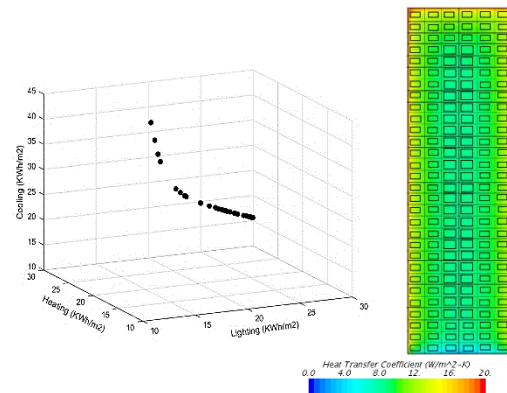


Figure 3: Pareto front for the triple-objective optimization for the case of room at the 15th floor located at the center zone of the building

Meseret Kahsay / mkahsay@uwo.ca
Girma Bitsuamlak / gbitsuam@uwo.ca
Fitsum Tariku / Fitsum_tariku@bcit.ca

Incorporating improved computational wind engineering into hybrid testing of wind turbines

Experimental testing of wind-loaded industrial wind turbines is quite challenging as the wind turbine blades are Reynolds number-dependent. Alternatively, hybrid simulation can be used to incorporate numerically calculated blade loads into experimental studies of wind turbines. However, due to hybrid testing's lack of maturity for studying wind-loaded structures, the current methods of numerically generating wind loads during hybrid testing have room for further development.

Typically, 2D-based methods like the blade element momentum technique are used to numerically calculate wind loading on turbine blades due to their computational efficiency. Since they're 2D-based, however, they can't capture the full 3D aerodynamic behaviour of wind flow around turbine blades. Swapping to the more robust computational fluid dynamics (CFD) should improve these results at the cost of increased computational demands.

Thus, a hybrid testing framework will be developed using CFD simulations and validated using a full-scale test of a micro turbine at WindEEE.

Firstly, CFD simulations of wind turbine blades (Fig. 1) will be used to train a surrogate model that associates blade position and incoming wind with the resulting structural loads. Then, this framework will be applied to a hybrid test of a micro wind turbine equipped with damper (Fig. 2b). Hybrid tests using the old framework and the new will be contrasted, and wind tunnel data will act as the baseline.

The target micro wind turbine for this test has a hub height of 1.7m and a blade diameter of 2.2m. While it has been previously studied in the BLWTL tunnels, it had a notable amount of blockage of the wind flow. WindEEE, by contrast, represents a larger facility where synoptic winds can be applied to this full-scale micro turbine (Fig. 2a). The results of this testing will

act as the baseline for the hybrid testing described above, validating and quantify any improvements offered by the newly developed framework.



Figure 1: CFD mesh of a wind turbine blade

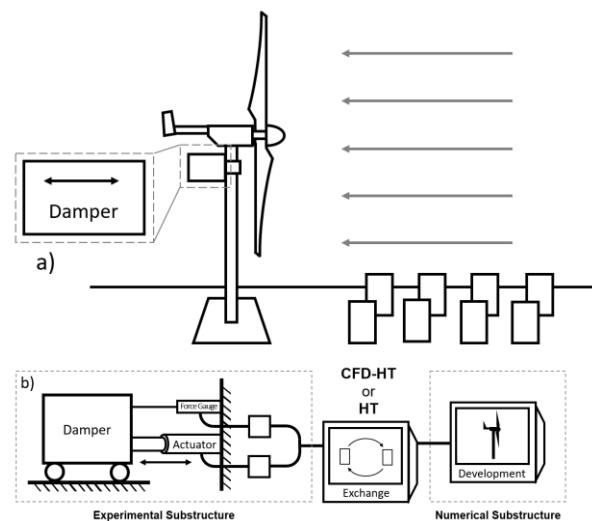


Figure 2: Proposed wind turbine WindEEE experiment (a) and hybrid test (b)

Eric Rowland Lalonde / elalond3@uwo.ca

Girma Bitsuamlak / gbitsuam@uwo.ca

Kaoshan Dai / kdai@scu.edu.cn

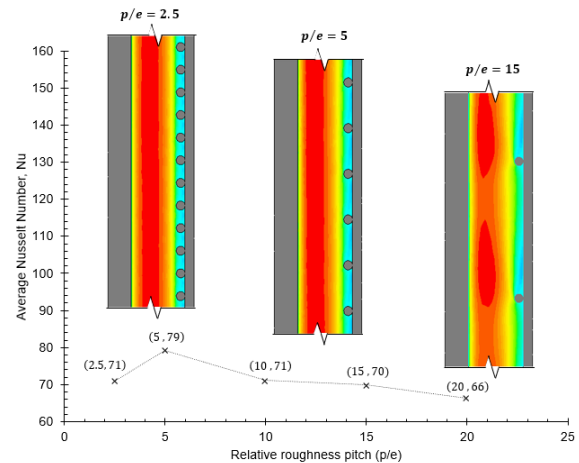
Numerical investigation of the obstructed flow and heat transfer characteristics in the air channel of a building integrated photovoltaic/thermal envelope system

Traditional building envelope systems serve to provide the basic control, support, finish, and distribution functions. In view of sustainability, these functions can be extended to include generating and harnessing energy. This is the premise for design and adoption of Building Integrated Photovoltaic and Thermal envelope (BIPV/T) systems. The BIPV/T envelope are relatively more cost-effective in that the PV support systems are eliminated.

However, overheating of the PV is a concern due to the constricted air flow passage behind the PV. Hence, an effective cooling strategy that incorporates a combined refrigerant tubes fitted behind the PV panels and an airflow passage is proposed. The heat extracted will serve to offset the heating demand of the building. The refrigerant tubes will be part of a heat pump cycle to improve the usefulness of low-grade thermal energy. Given the complexity of the BIPV/T system, the operation of the system is ensured by an effective control system that provides three cooling scenarios: (a) Case I: Refrigerant cooling with buoyancy driven flow in the air channel; (b) Case II: Refrigerant flow and forced flow in the air channel; and (c) Case III: Refrigerant flow and forced flow such that the building exhaust air is used to evaporate the refrigerant. Case III will ensure year-round operation of the BIPV/T system.

It is therefore important to understand the heat transfer and pressure loss characteristics for each of the cooling strategies. The findings from investigating the Case II cooling scenario is herein presented. The study is conducted using CFD code. It should be noted that the numerical model was simplified such that the refrigerant tubes are treated as transverse rib elements. The impact of the geometric parameters on

the thermo-hydraulic performance is studied. These parameters include relative roughness height (e/D_h) and relative roughness pitch (p/e). The figure shows that there is an optimum p/e for which the heat transfer is maximized.



Barilelo Nghana / bngghana@uwo.ca

Fitsum Tariku / ftariku@bcit.ca

Girma Bitsuamlak / gbitsuam@uwo.ca

Finite element modelling of low-rise building response to tornado loads

Tornadoes are an extreme weather phenomenon that can cause severe damage to communities. In the United States, over 1000 tornadoes occur annually [1] that can cause significant damage and risk to human life, such as the April 2011 “super outbreak” that resulted in \$11 billion in damage along with 321 fatalities [2]. Canada also experienced around 60 verified tornadoes annually [3], with a notable event being the 2018 Dunrobin tornado that caused \$300 million in insured losses [4].

There is a growing interest in modelling the behavior of structures under tornado wind loads. Numerous studies have been conducted to evaluate the pressure distribution on structures subjected to tornado loads, done both experimentally and numerically [5]. There have also been full scale studies conducted to evaluate the damage caused by severe winds, which are costly to conduct [6]. Using coupled approach with finite element analysis and computational fluid dynamics (CFD), the aim of my research is to numerically model the structural response of a building subjected to tornado loads.

The pressure distribution on typical low-rise structure has been simulated using CFD. The study involved varying tornado flow parameters, such as the swirl ratio, and the building’s location relative to the vortex. CFD simulations will also be developed to capture transient effects such as peak wind speeds along with translating tornado vortices.

Going forward, an accurate finite-element model of a low-rise building will be developed and subjected to loads from tornado vortices in order to determine the structural response. The variance of tornado size and intensity along with the building’s location with respect the tornado will be incorporated to observe changes in wind pressures and response of the building. Validation of the numerical model is also

expected to be coupled with experimental tests at the WindEEE Dome.

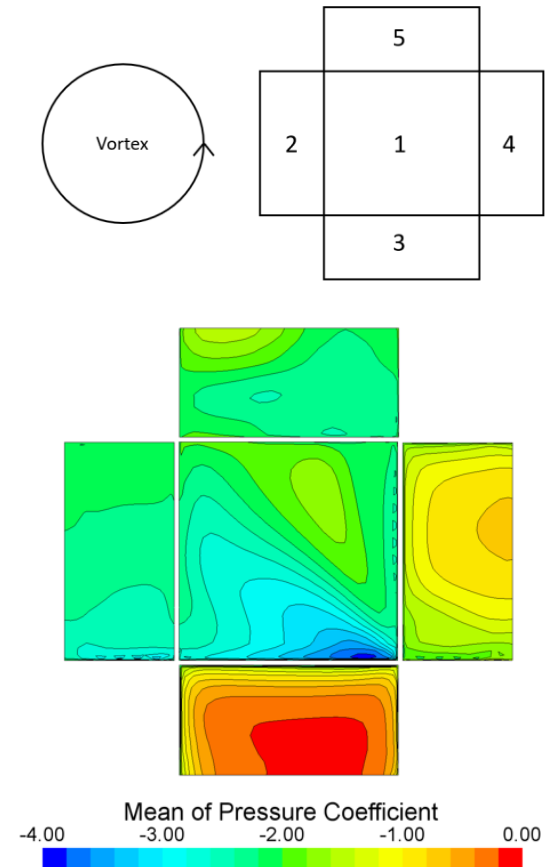


Figure 1: Pressure distribution on a square low-rise building placed at the location of maximum wind speed in a tornado-like vortex

Cody Van Der Kooi / cvande89@uwo.ca

Girma Bitsuamlak / gbitsuam@uwo.ca

BIM integrated sustainable and resilient building design for northern climate

Canada's Arctic and northern residents have for long time suffered from the lack of many opportunities, services, and standards of living as other Canadians enjoyed. These northern communities therefore experience many concerns to sustain themselves, in which housing represents one of the major ongoing problems. Many of current houses are poor quality and have not considered harsh climate conditions in northern Canada (i.e. 90% of Nunavik population live in unsuitable houses). For instance, structural damages, systemic problems like permafrost degradation, mold and accelerated deterioration, and relying on the fossil fuel as a primary source of energy for thermal comfort.

An improved understanding of building adaptation in the Canadian North has become a vital requirement for sustainable and resilient northern communities. Buildings in the north are subjected to extreme environmental stressors: above-grade thunderstorms, snow, extreme wind, rain, thermal stress and sub-grade permafrost degradation due to climate change and local urban activities. Further, Arctic buildings are losing enormous energy through exposed building enclosure that warrants realistic environmental load considerations.

One approach to change the traditional building design to building-based adaption design perspective is performing numerical and experimental simulation that identifies and examine the conceptual relation between Arctic buildings and microclimate. This method involves developing numerical models that mimic the wind flow, the heat transfer and snow deposition around the building(s).

This project proposes a framework that identifies and examine the conceptual relation between building performance and climate loads from the perspective of energy efficiency, permafrost degradation, and wind loading. This in turn helps promoting a concept

of building-based adaption design for northern climate.

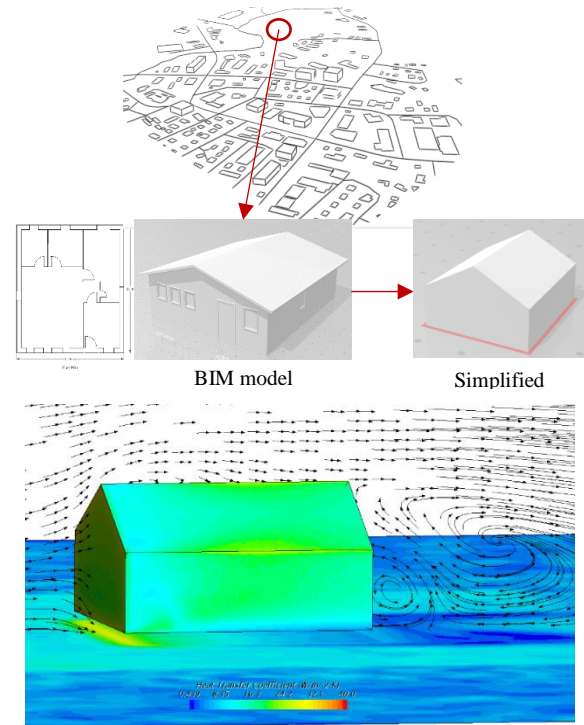


Figure 1: Wind field vector and CHTC contours

Muna Younis / Myounis4@uwo.ca

Girma Bitsuamlak / gbitsuam@uwo.ca

Effects of city growth on tall building cladding fatigue

Fatigue damages of building cladding and component due to wind loads is of great interest. Cladding fatigue analyses in published literature have been focused on low-rise building, especially in locations such as roof corners where pressure fluctuation tends to be intensive. However, very few investigations have been conducted on high-rise building cladding components, which are made of glass curtain walls with metal connections on most modern skyscrapers. Like low-rise building aerodynamics, air flows detach at the sharp edges/corner, which results in high negative pressure zones with great amount of pressure fluctuations. Before these fluctuations get transferred into the structural members of the building, the stresses are first taken by claddings on the facades. With significant number of cyclic loadings applied on the walls, their connections will likely suffer from fatigue damage as time passes. In this study, the impact of city growth (and hence increased turbulence) on cladding fatigue.

The wind load data used in this study is taken from the experimental results of the OCE/NSERC-CRD and SOSCIP joint research project whose objective was to determine the effects of city growth. By courtesy of this research project, the wind pressure time-history data are taken into this study to estimate fatigue damages induced by wind.

In the fatigue analysis, the C_p time-histories are counted as C_p cycles with difference ranges and means, using Rain Flow Counting Algorithm. Once the C_p cycle histogram is produced, the same histogram can be applied to different mean wind speed, with the difference of total cycle per unit time. Then, when knowing a suitable mean wind speed distribution model for the location, corresponding time periods for different mean wind speeds can be determined in a certain life span (e.g. 10 years). Next, by summing up the resultant pressure cycles under each wind speed strip, the overall cycle histogram in this life span can be produced. In the end, using the material

property of the design connection, combined with miner's law (cumulative damage) and Goodman's approach (mean stress effect), the total fatigue damage can be determined. Applying the same procedure for five different surrounding intensity representing city growth instances, different damage patterns around the facades can be plotted and compared

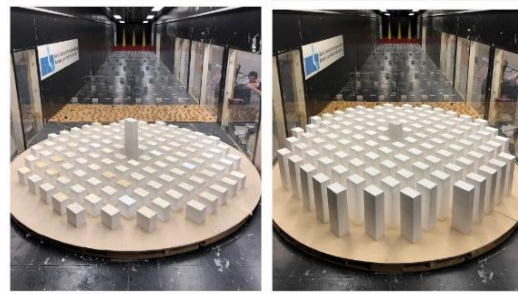


Figure 1: Wind tunnel test setup

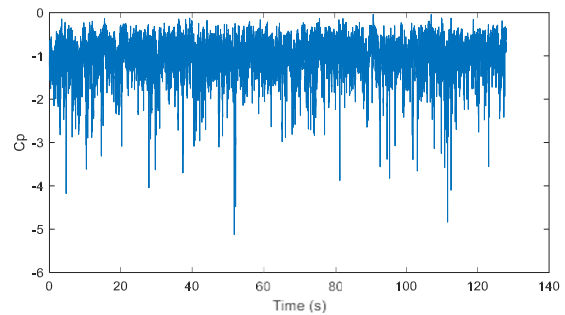


Figure 2: C_p Time History

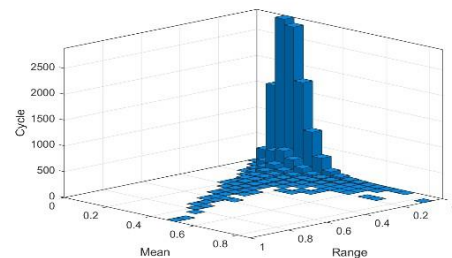


Figure 3: C_p /Stress Cycle Histogram

Hang You / hyou24@uwo.ca

Ayan Sadhu / asadhu@uwo.ca

Girma Bitsuamlak / gbitsuam@uwo.ca

Dynamic analysis for a negative-Gaussian curvature cable dome

During the last decades, most architectures has adopted the use of cable structures for covering large areas such as arenas, stadiums and open squares because of their lightweight and versatile forms. Cable domes are considered one of the most widely used cable structures in practice. However, research is needed to understand the wind behavior of these structures. The current research involves investigating the wind-induced response of cable roofs, considering the influence of curvature and flexibility. The study will focus on doubly curved cable domes which have better stability than the corresponding positive-curvature cable domes and better stiffness than cable net structure.

The large deformations of this type of structures require considering the interaction that occurs between the structure deformations and the wind forces. This will be carried out experimentally using wind tunnel testing and numerically by coupling Computational Fluid Dynamics and Finite Element Modeling.

The study will also involve the development of coupled finite element-optimization technique that can be used to determine the optimum cable shape and the pre-stressing cable forces that achieve the best aeroelastic behavior of doubly curved domes.

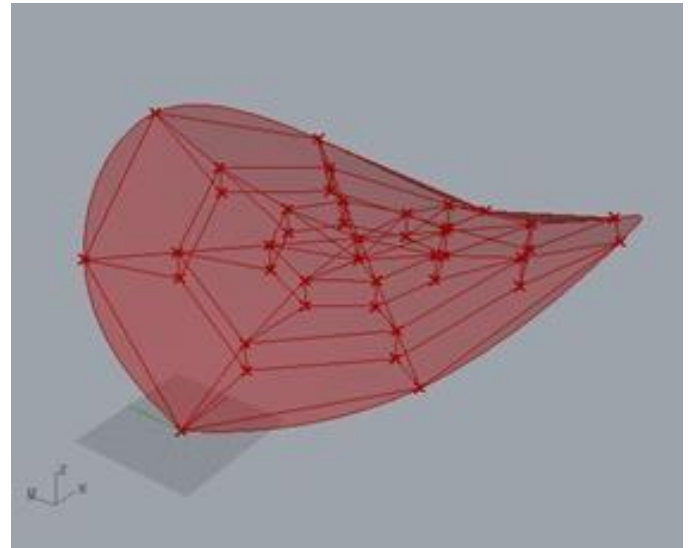


Figure 1: 3D view of a negative-Gaussian curvature cable dome



Figure 2: The largest cable dome: Georgia Dome

Elshaimaa Ahmed / eahmed23@uwo.ca
Ashraf El Damatty / damatty@uwo.ca

Analysis of mid-rise timber buildings

Heavy timber has been gaining strong popularity worldwide. The use of heavy timber has been increasing exponentially due to its improved properties over light frame wood structures. The objective of this study is to assess, the structural behaviour of various heavy timber systems used in a multi-storey building in comparison with the light-frame wood (LFW) system.

The reference structure is a real 4-storey L-shaped LFW building recently constructed in Canada. The same building layout is remodeled and redesigned using four different heavy timber structural systems: Moment resisting frames (MRF), braced frames (BF), and shear walls using Cross laminated timber (CLT) panels. The four structural systems are numerically modelled. In order to be able to compare between the different systems, the layout and dimensions of the structural system of the three heavy timber buildings are selected such that those buildings have almost the same lateral stiffness as the reference LFW building.

The four numerical models are exposed to the same gravity and wind loads according to the NBCC. Also, wind tunnel test data are considered for application to the mid-rise structures using a nonlinear time-history analysis. A key element that governs the behavior of timber structures is the connection between various elements. Connections with known mechanical characteristics based on test results available in the literature are used in the study. The choice of the members of the heavy timber systems is restricted to those used in the tested connections. In addition, all members are designed to satisfy the strength requirements under the combined effects of gravity and lateral loads.

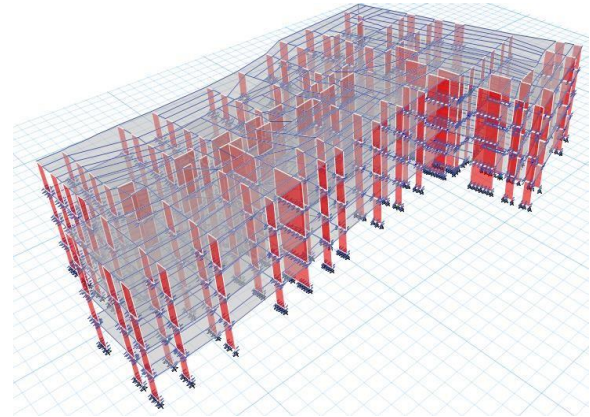


Figure 1: Numerical Model Showing the formulation of CLT Panels as shear walls.

Moustafa El-Assaly / melassal@uwo.ca

Ashraf El-Damatty / damatty@uwo.ca

Behavior of transmission line structures under tornado-induced wind loads

Tornadoes, referring to swirling high-intensity winds, are a major threat to transmission line infrastructure worldwide. The United States and Canada are among the most active zones for tornadoes. Failures of transmission lines during tornadoes have been occurring more frequently, especially in Ontario, including incidents near Sarnia in 2003, 2006, and 2011, near Wawa in 2013, Woodstock 2016 and Ottawa 2018. Considering these facts, a comprehensive study has been triggered to mitigate such failures. The research includes numerical and experimental simulations of tornadoes and transmission line structures.

Using numerical simulations, structural response of a multi-span self-supported transmission line system under various mid-range tornadoes are investigated. Nonlinear three-dimensional finite element model is developed for both systems. Computational fluid dynamics (CFD) simulation is used to develop the matching tornado-like vortices. Using proper scaling approach for geometry and velocity, full-scale flow fields of various F2 tornadoes are simulated. The velocity fields are incorporated in the three-dimensional finite element models. Sensitivity analysis is conducted to assess the variation of the members' peak forces associated with the location of the tornado relative to the transmission line.

The transmission tower members' peak internal forces due to various tornadoes are compared with corresponding values evaluated using the ASCE-74 manual of practice, which currently do not account for tornado-induced loads.

In addition to the mentioned parameters, there are several significant factors considering the tornado performance of transmission line systems and potential causes of past failures which are still unknown, namely dynamic effects, shielding effect on lattice transmission tower under non-synoptic

tornado wind, fluid-structure interaction and experimental validation of the finite element model of transmission line structures under tornadoes. To address these currently unknown factors of transmission lines behavior under tornado wind fields, an extensive set of integrative experimental examinations is conducted in WindEEE Research Institute.

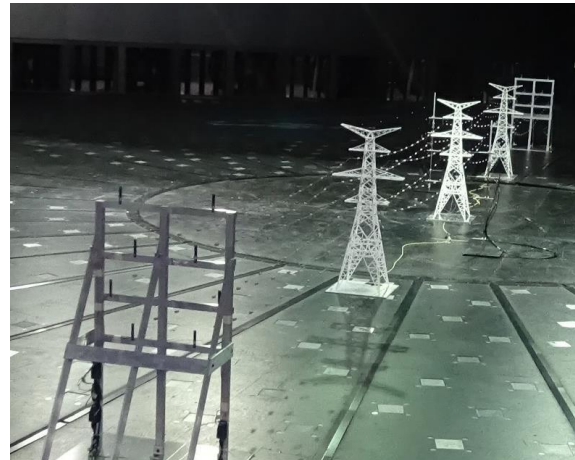


Figure 1: Aero-elastic transmission model



Figure 2: Full aero-elastic transmission line model under a simulated tornado conducted in WindEEE research institute

Nima Esami / nezami@uwo.ca

Ashraf El-Damatty / damatty@uwo.ca

Numerical model for analysis of wind turbines under tornadoes

According to the Global Wind Energy Council, the installation rate for wind turbines is accelerating around the world, leading to the introduction of new wind turbine farms in regions where wind is abundant. As a result, the number of wind turbine towers prone to severe wind loads is increasing, as is the rate of failure due to unexpectedly strong wind loading. Wind turbines are typically designed to resist the synoptic wind loads specified in current International Electro-technical Commission (IEC) guidelines, but these standards fail to include consideration of High-Intensity Wind (HIW) events such as tornadoes or downbursts. Because such HIW events stem from localized natural events, identifying critical locations that result in peak forces acting on the tower and blades is a challenging task. For this reason, a built-in-house numerical model has been developed for simulating a three-blade horizontal-axis wind turbine tower exposed to 3D tornado wind fields. An extensive study has been conducted with the goal of determining both the critical location of a tornado that will cause peak straining actions on the tower and blades, and the optimal pitch angle that will minimize the effects of that tornado.

The ongoing study resulted in the development and validation of a numerical model for predicting the response of wind turbines to tornado loading. The developed HIWWT numerical model incorporates a wind field that was generated from a previously developed CFD model. The analyses are based on moving the tornado in space around the wind turbine in order to determine the critical tornado locations for both the tower and the blades for a variety of blade pitch angles. The developed numerical model was applied for the tornado analysis of a case study of an actual wind turbine. It has been found that an F2 tornado wind field presents a hazard for wind turbine towers and must therefore be considered if the negative impact of this type of unexpected load on tower elements is to be avoided.

In the next step, the effect of tornado loads on tower's height and airfoil sections will be investigated. Alongside with studying the effect of different tornado wind fields on the tower and blades.

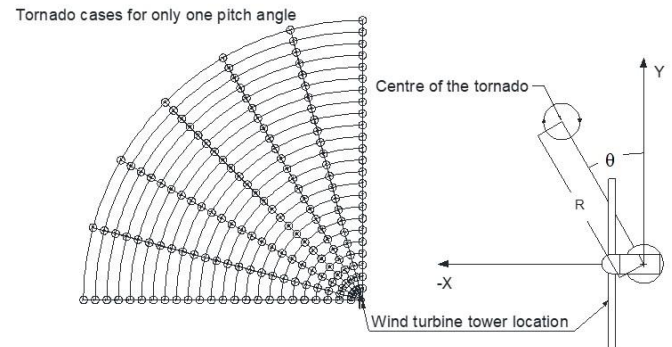


Figure 1: Schematic of tornado locations for the current study relative to the centerline of the wind turbine

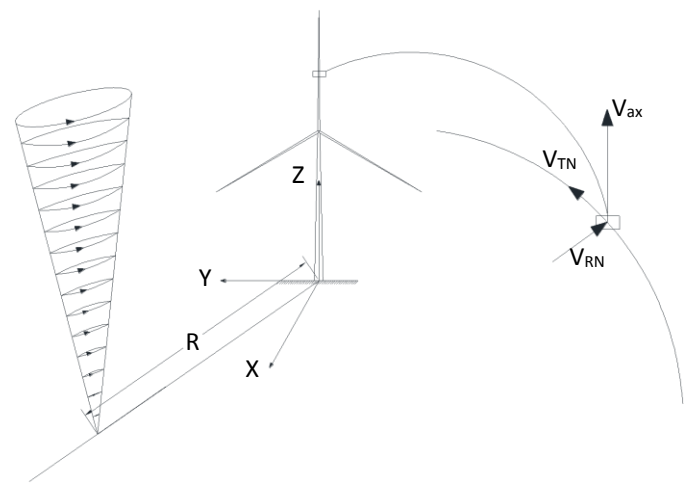


Figure 2: Velocity Components of the tornado wind field for a random element in the coordinate system.

Mohamed Abu Gazia / mabugazi@uwo.ca
Ashraf El-Damatty / damatty@uwo.ca

Angle and end transmission lines towers behavior under tornado wind loads

Electrical energy plays a vital role in many aspects of daily life. The United States of America and Canada are active zones for tornadoes with approximately 800 to 1,000 tornadoes per year. Sever wind events in the form of downbursts and tornadoes are referred to as High Intensity Winds (HIW). Such events are responsible for more than 80% of all weather-related transmission line failures worldwide. Despite this fact, the current codes of practice for transmission line structures do not account for wind loads resulting from tornado events. In these codes, the specified design wind loads are based on large scale storms with conventional boundary layer wind profiles. The forces acting on the structure depend on the location of the storm relative to the structure. Therefore, it is important to identify the tornado and downburst locations that lead to the maximum structural responses. This is challenging for transmission lines, where the wind forces resulting from tornadoes vary along the wing span of the lengthy conductors and along the height of the towers. Thus, the behavior of angle and end lattice transmission towers will be assessed under tornado wind loads. The research proposed in this study will build on the findings, developments and experience gained during the previous research program. The objective is to develop guidelines for designing transmission line structures to resist HIW events and to use these findings in codes of practice.

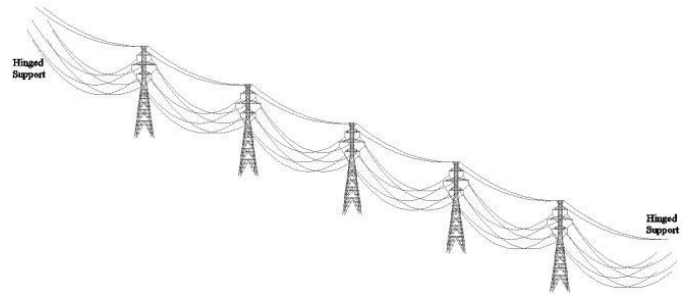


Figure 1: Schematic Layout of the transmission line system model

Mohamed Hamada / mhamada2@uwo.ca

Ashraf El-Damatty / damatty@uwo.ca

Progressive failure of self-supported transmission line towers under different tornado wind fields

Transmission line (TL) structures play an essential role in delivering electricity. The collapse of these structures can cause substantial economic and societal losses. Most weather-related failures of TLs are caused by High-intensity wind (HIW) events such as downbursts and tornadoes. This research adds to the existing research on mitigating the failures of TLs due to tornadoes.

This study investigates the progressive failure of single TL towers as well as TL systems under different F2 tornado wind fields. In order to achieve this goal, different tornado wind fields are incorporated in a fluid-structure software that is developed and validated at Western University. The software is utilized to conduct an extensive parametric study that identifies the most critical tornado configurations for a sample of four as-built guyed and self-supported TLs. Accordingly, progressive failure analysis is performed for these towers under the most critical tornado configurations. Moreover, strengthening of the TL towers to sustain F2 tornadoes is attempted to get an insight into the cost associated with designing TL towers to sustain F2 tornadoes.

The progression of failure within self-supported TL systems under different tornadoes is then investigated. Finally, the effect of changing the insulator length as well as the span of the TL on the propagation of failure within TL systems is examined.

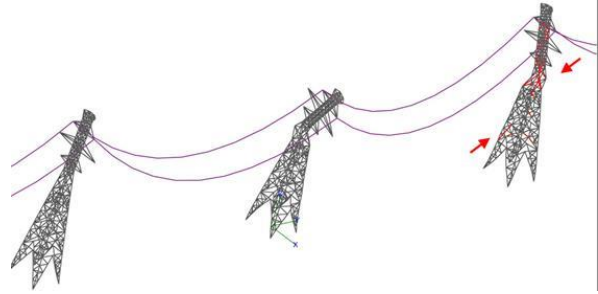


Figure 1: Propagation of failure within self-supported transmission line systems subjected to tornadoes

Wesam A. Mohamed / wabdelha@uwo.ca

Ayman El Ansary / aelansa@uwo.ca

Ashraf El Damatty / damatty@uwo.ca

Shear buckling testing of wood sheathing panel

Wood-based sheathing panels are common to be used in the light-frame wood (LFW) construction due to their relative in-plane stiffness to resist lateral loads. The typical size of the sheathing panel in the construction industry is 1220×2440 mm and panels are connected to studs and plates by nails. One of the failure modes of LFW shearwall segments under lateral loads is the out-of-plane deformation of sheathing panels while the nail-based connections do not reach their ultimate capacity. The experimental research on this topic is limited to the small size of the plywood and different edge loads. The early research on buckling strength of plywood sheathing panels with simply and fix supported boundaries under compression loads was conducted to verify the usual buckling theories with some design recommendations [1]. The shear buckling of plywood panel with 1220×1220 mm and 610×1220 mm dimension which is subjected to diagonal compression force was carried out to determine the shear resistance of a typical farm diaphragm segment [2]. Another experiment was conducted by [3] to identify shear stress distribution and shear characteristic in wooden glued thin plywood panels (<5.5 mm) with square shape.

The current Canadian Wood Design code (CSA O86-14) presents the usual buckling theoretical equation for determining the critical shear stress for a sheathing panel with simply supported boundaries along all edges with the assumption that the sheathing panel is experiencing uniform shear stress along the edges and the contribution of intermediate studs is neglected [4].

The shear buckling test will be carried out in a specially designed frame at the structural laboratory at the Department of Civil and Environmental Engineering, Western University. The figure shows the designed frame layout. The objective of the current research is to assess the buckling behavior of

wood-based sheathing panels with intermediate and edge intermittent nail supports subjected to pure shear. In addition, the post-buckling performance of wood sheathing panels is investigated.

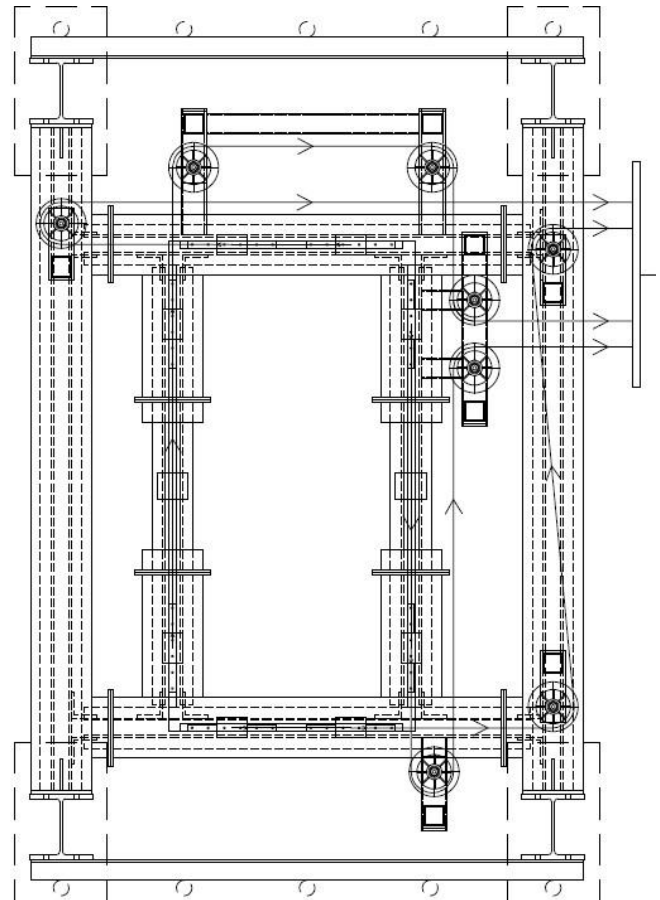


Figure 1: Plan view of setup for shear buckling test

Mohammad Niazi / mniazi6@uwo.ca

Ashraf El Damatty / damatty@uwo.ca

Detailed and simplified numerical analysis of multi-story light-frame wood buildings

About ninety percent of North America's residential buildings consist of light-frame wood structures (LFWs). Being an environment-friendly material, wood is becoming more popular in midrise building construction around the world. The National Building Code of Canada NBCC 2015 allows up to six storeys of LFWs, an increase from the previous code provision that limited LFWs to four storeys.

A recently proposed LFW finite element modelling (FEM) procedure was applied to a real four-storey three-dimensional building. This very detailed model simulated all nails, frame members and sheathing panels for all the walls of the building. This tremendous effort was carried out to study the structural behaviour of a three-dimensional LFW building with the consideration of system effect, and to have a benchmark model that can be used for validation of simpler models. Detailed modelling of all components for all walls of a three-dimensional building is not practical. A simplified FEM procedure was developed based on replacing the individual shear wall with flexural and shear nonlinear springs with properties obtained from matching flexural and shear deformations to those of the detailed model. Moreover, ambient vibration measurements were conducted for the building to determine its fundamental period. Verification of the accuracy of the detailed model was undertaken by comparing its result with field measurement in terms of fundamental period. Also, pushover curves obtained from both the simplified and the detailed models were compared. It was demonstrated that the simplified FEM can predict pushover curve for single wall and multi-story three-dimensional buildings with very good agreement to those predicted by the detailed FEM.

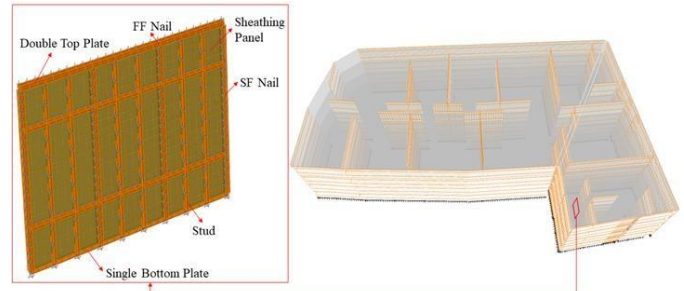


Figure 1: Detailed numerical model of the LFW building

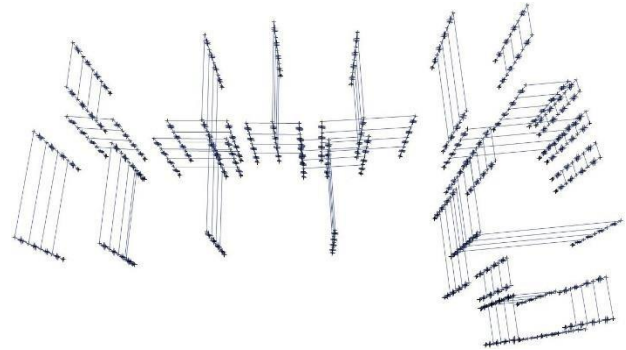


Figure 2: Simplified numerical model of the LFW building

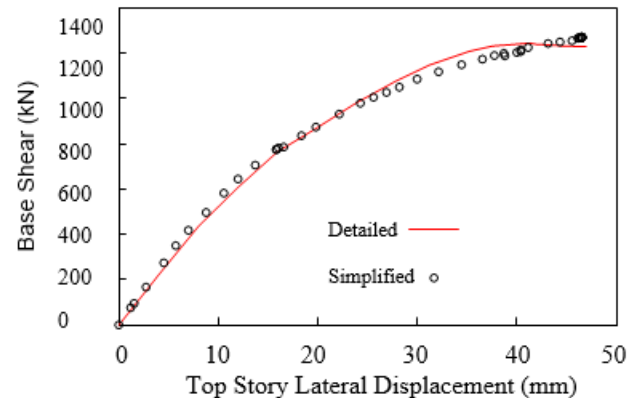


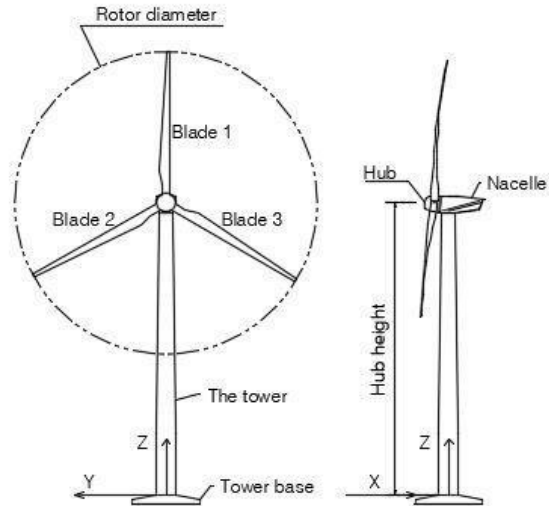
Figure 3: Comparison of pushover analyses results for both the detailed model and the simplified model of the LFW building

Chu Peng / cpeng52@uwo.ca

Ashraf El-Damatty / damatty@uwo.ca

Behavior of wind turbines under downburst wind loading

A numerical model is developed to study the performance of wind turbines under downbursts. The numerical model simulates both the wind turbine tower and the blades and incorporates downburst wind fields based on Computation Fluid Dynamics (CFD) simulations. The model considers the variation of the location of the downburst relative to the tower as well as the variation of the blades pitch angles. After validating the numerical model, a real wind turbine is considered for analysis. An extensive parametric study is conducted to determine the peak moments at the tower base and the roots of the blades considering 38,808 load cases including 5,544 downburst configurations for 7 different blades pitch angles. Critical configurations of the downburst which produce maximum stringing actions on the tower and blades for different blades pitch angles are identified. The optimum blade pitch angle which minimizes the downburst effect on both the tower and the blades is then determined. The maximum downburst jet velocity that the tower and the blades can sustain compared to the criteria used in currently design codes and guidelines is estimated. The study emphasizes the importance of considering downbursts in the structural design of wind turbines. Downburst design criteria and critical wind profiles are currently under development.



Mostafa Ramada / mramada2@uwo.ca

Ashraf El-Damatty / damatty@uwo.ca

Cascade failure of transmission towers along a line subjected to downbursts.

Transmission line's cascades have played a major role in several serious accidents around the world, as they are particularly prone to occurring in the presence of strong winds. The failure of a line component overloads the system, inducing a progressive failure that can involve many transmission line (TL) supports. Due to their localized nature, downbursts cause unequal wind forces on various towers of a transmission line; the collapse of one tower can affect the adjacent towers through the unbalanced forces that develop in the conductors, which can lead to a cascaded-type of failure along the entire line. Research related to high intensity wind loads and their effects on structures in general is very limited and on transmission line structures is rare. Previous failure investigations were limited to individual towers. However, an incremental progressive failure analysis must be considered since failures of transmission lines occur in the form of a cascade failure progressing from one tower to another. Therefore, a nonlinear finite element model was developed to assess the capacity of transmission lines under downbursts. The numerical model can predict (i) the tower's post failure geometry by capturing the plastic hinge formation and the failure mechanism until a state of equilibrium occurs (ii) the tension developed in the new conductor's profile by utilizing the extensible catenary approach in solving three-dimensional conductors with moving boundary conditions under horizontal and vertical loads.

In the next step, a model will be tested at WindEEE Dome at Western University for the validation of the progressive failure model in order to understand the failure mechanism of the entire line.



Figure 1: Progressive failure of Transmission lines occurred in South Australia during Sept 2016 Thunderstorms

Ahmed Shehata / ashehat7@uwo.ca
Ashraf El-Damatty / damatty@uwo.ca

Environment: Biofixation of carbon dioxide

Photosynthetic carbon capture by trees and other vegetation is believed to be among the most efficient and environmentally friendly strategies to reduce CO₂ concentration in the earth atmosphere. The 2018 IPCC special report suggests that 1 billion hectares of new forest is necessary to limit global warming to 1.5 °C by 2050. However, recent studies estimate that only 0.9 billion hectares of land are available on the earth outside of cropland and urban regions for potential forest restoration. Water availability can also be one of limitations of this strategy. Biofixation of carbon dioxide by aqueous suspensions of bacteria and algae (referred to as living or active fluids) is an alternative solution for limitation of CO₂. Biofixation is 10–15 times more efficient than trees and produces biomass that has value in producing biofuels, human nutritional supplements, cosmetic products, biofertilizers and animal feed. These microorganisms are cultivated in dedicated reactors commonly referred to as photobioreactors (PBR).

In this research we study the phototaxis behavior of *Synechocystis* sp.PCC 6803, a model micro-organism to study photosynthesis. We have previously characterized the intermittent motility of these bacteria, based on the alternation of “run” periods during which they move, and “tumble” periods that consist of localized motion (Figure 1). We track the bacterial response to light stimuli, under isotropic and non-isotropic (directional) conditions. We investigate how the intermittent motility is influenced by illumination.

The photosynthetic micro-organisms are sensitive to light intensity and can adapt their diffusion by triggering the characteristic times of their intermittent motility. With higher illumination, bacteria have a greater propensity to be in a run mode during which they perform longer displacements and therefore increase their diffusion coefficient (Figure 2-a).

We model analytically the response of *Synechocystis* cells by using the linear response theory. A response function that has been proposed to describe *E.Coli* chemotaxis was found suitable to fit our experimental data, with an adaptation of the numerical values of the response function parameters.

Under directional light flux, *Synechocystis* cells perform a phototactic motility and head toward the light source. This biased motility stems from the averaged displacements during run periods, which is no longer random. We show that the bias is the result of the number of runs, which is greater toward the light source, and not of longer runs in this direction. Brought together, these results suggest distinct pathways for the recognition of light intensity and of its direction in this prokaryote micro-organism, that can be used in the active control of bacterial flows (Figure 2-b).

In conclusion, we find that just after a rise in light intensity, the probability to be in the run state increases. This feature vanishes after a typical characteristic time of about 1 hour, when initial probability is recovered. Our results are well described by a mathematical model based on the linear response theory.

When the perturbation is anisotropic, we observe a collective motion toward the light source (phototaxis). We show that the bias emerges due to more frequent runs in the direction of the light, whereas the run durations are longer whatever the direction. This information is of primordial importance in hydrodynamical and radiative design of high performance photobioreactors.

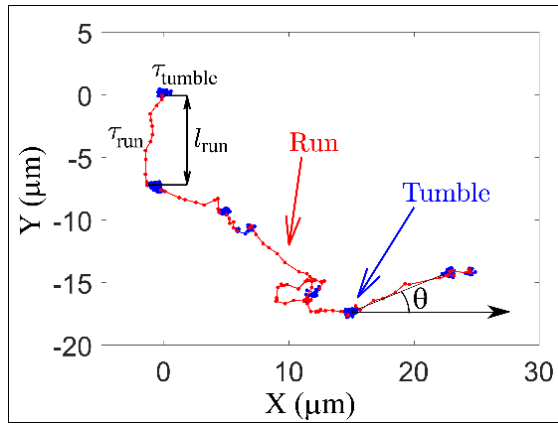


Figure 1: Trajectory of a bacterial cell (668 s). Runs correspond to red lines and tumble to blue dots. For the phototaxis assay, we define the angle between the direction of the run and the direction towards the light source, which is indicated by the arrow.

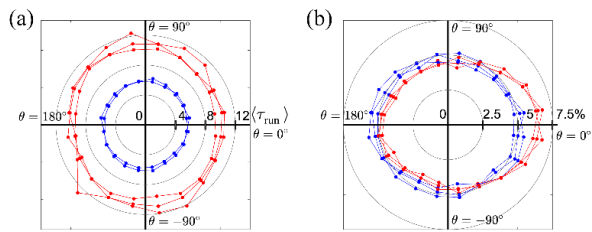


Figure 2: Average run (a) durations and (b) frequencies as a function of their angular directions, $\theta = 0^\circ$ being the direction towards the light source. Red: light source is turned on, blue: light source is turned off.

Thomas Vourc'h / thomas.vourch@gmail.com
Hassan Peerhossaini / hpeerhos@uwo.ca

Optimization of porous medium for solar radiation capture

Fossil fuel usage is resulting in global warming. There is a need to switch to renewable energies, but existing technologies lack the efficiency for wide-scale adoption. Concentrated solar power (CSP) is a renewable energy that could aid in the transition to a low carbon future by harvesting the abundant heat from the sun. CSP directs sunlight to a single focal point which is used to create energy. A challenge with the current design is that the surface of the thermal receiver reaches a high temperature and does not efficiently transfer the heat due to re-radiation losses. There is a need to re-design the thermal receiver to maximize the efficiency of CSP.

This project investigates the impact that varying the porosity of a thermal receiver would have on the efficiency of solar radiation heat capture. An experimental setup was created that would hold aluminum mesh under a halogen lamp. The temperature of the aluminum mesh was measured using a FLIR infrared thermal camera. The 3 mesh sizes measured had porosities of 5 PPI, 10 PPI, and 20 PPI. For accurate readings, the metallic mesh was painted with high temperature black spray paint. The mesh temperature was measured individually and while stacked. Results showed that the 5 PPI mesh had the lowest temperature, likely because radiation passed directly through. The 10 and 20 PPI mesh both had higher temperatures, with similar trends. Stacking the mesh was not the best configuration for heat to be effectively transferred from one block to the other, as large temperature differences were observed between the blocks. Figure 1 shows the temperature gradient measured in the individual mesh blocks. **Error! Reference source not found. 2** hows the measured temperature gradient in the stacked mesh blocks. As it can be seen, the temperature at the surface is still very high compared to the lowest block, with large differences in temperature between the individual blocks. It is theorized that a design with gradually changing porosity will provide better heat capture.

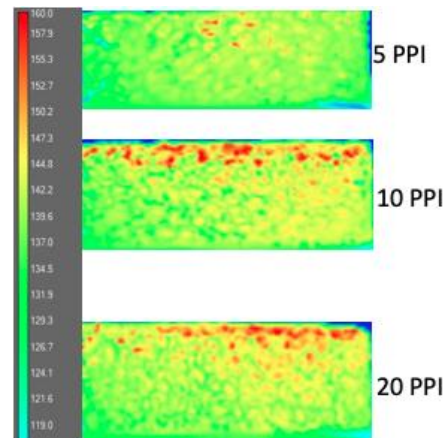


Figure 1: Individual mesh temperatures

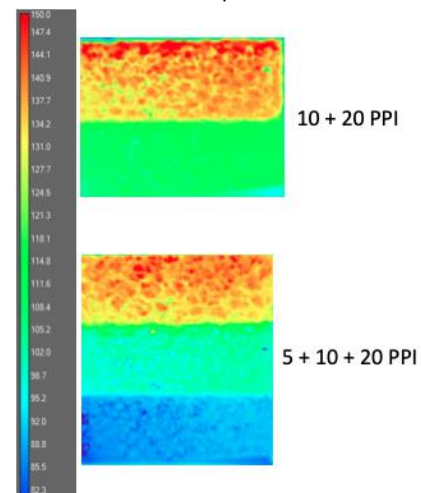


Figure 2: Temperature results for stacked foam

To analyze heat capture in porous media, a computational model will be created and validated against a simple experimental model. This experiment measures the temperature of an aluminum block with a drilled hole that has a gradually decreasing diameter down the block. In the side of the block, there are small holes through which the temperature can be visualized with a FLIR infrared camera. Temperature results will be analyzed and compared to the computational model. Adjustments will be made to the computational model to match the experimental results. Once the computational model is validated, the design will be modified and tested to optimize radiation heat capture.

Elizabeth Blokker / eblokker@uwo.ca

Kamran Siddiqui / ksiddiq@uwo.ca

The Development of an optical guide system for parabolic dish solar concentrators

Solar thermal systems have been a heavily discussed topic over the years, with one system of interest in thermal engineering being the Parabolic Dish Concentrator. By concentrating incident sunlight rays to a single spot, the thermal intensity of the receiving solar energy is magnified many times over with each mirror (or lens) posing as a single sun shining directly at the same focal point on the dish, resulting in higher overall power per square meter of dish. The reception of this energy is traditionally done with a sterling engine but produces a low efficiency as a result of the heat transfer fluid's thermal losses. It is because of this that a proposed optical guide is being designed in order to directly reflect the sun's rays to a receiving point, eliminating the need for a heat transfer fluid.

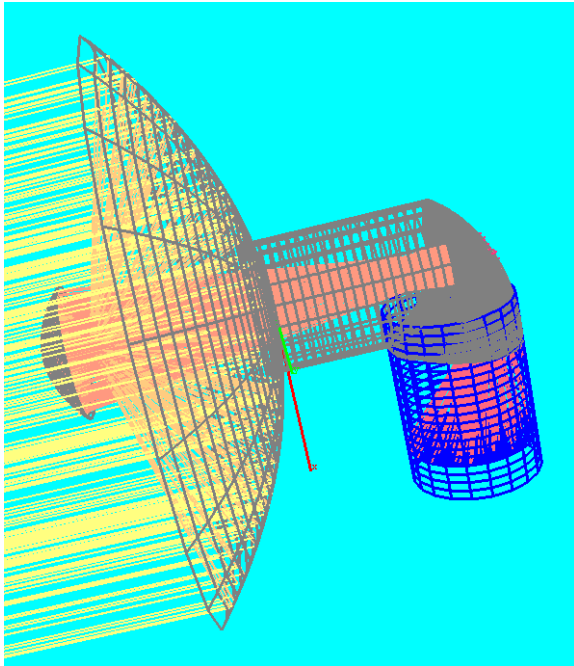


Figure 1: Dish Native Orientation

Development of the optical guide starts with computational modelling done through a ray tracing program which utilizes a Monte-Carlo Ray Tracing algorithm (MCRT). This algorithm integrates all ray intersections arriving to a single surface point and

adjusts the flux value based on the surface's absorptivity. A model was created with a primary parabolic reflector and a secondary parabolic reflector which uses the secondary reflector to concentrate rays through an aperture in the first. The rays through this aperture then strike a mirror that reflects incident energy into the optical guide and ultimately a receiving material (Figure 1).

Current work includes the modelling of several incident angles that must be taken into consideration, as variance in these angles result in the need to adjust the guide mirror's angle in order to correctly direct rays to the receiving material (Figure 2). Flux distributions developed on the receiver are of extreme interest as a perfectly radial uniform distribution will lead to the most effective optical guide design. Different positions and geometries of optical guides are currently being developed to produce the most favorable distribution on the receiver.

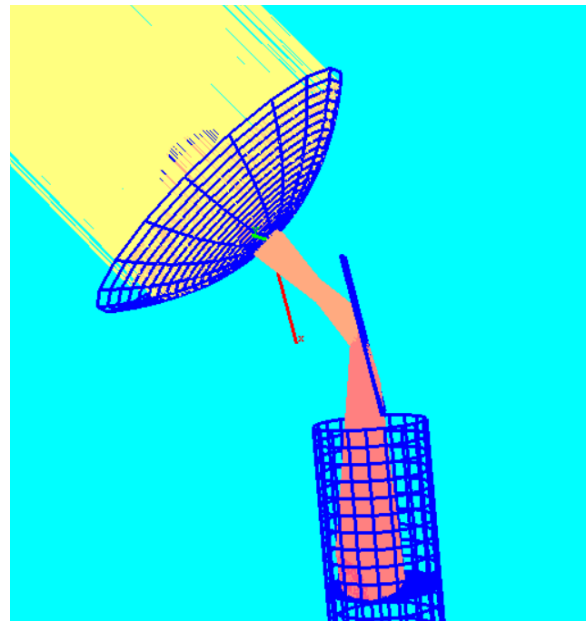


Figure 2: Varied Incident Angle Orientation

Zane Charran / zcharran@uwo.ca
Kamran Siddiqui / ksiddiq@uwo.ca

The influence of wall heating on turbulent bursting and sweeping phenomena in the turbulent boundary layer

In many engineering and environmental applications, the boundary layer encountered is turbulent and involves heat transfer. The atmospheric boundary layer is one such application in the field of wind engineering. In this flow, heat transfer from the Earth's surface into the atmosphere drives the buoyant force to interact with flow inertia and the viscous shear force. It is of interest to wind engineering field to study the interaction of these forces as it greatly influences the transportation of heat, momentum (e.g. dynamic wind loading on structures) and species (e.g. greenhouse gases and particulate matter) through the boundary layer. Turbulent burst and sweep events are unique phenomena where low momentum fluid close to the wall is ejected upward and a sweep event occurs where high momentum fluid relatively far away from wall suddenly rushes towards the wall. These events are known to drive substantial local stress and contribute significantly toward the net transportation of momentum, heat, and species. The objective of this research is to characterize the modification of these turbulent phenomena by wall heating.

Experiments are performed in a closed loop low-disturbance wind tunnel. The test section is 46 cm by 46 cm in cross section and 114 cm long with walls made of clear acrylic for visualization. The smooth horizontal bottom wall is unheated or heated between 45 °C and 90 °C while the free stream velocity was held constant at ≈ 7.5 m/s to study the flow behavior. The multi-plane PIV technique was used to capture two-dimensional velocity fields in vertical (x-z) and cross (y-z) planes.

Turbulent burst and sweep events were detected utilizing a quadrant analysis where each turbulent velocity vector is decomposed into one of four unique quadrant events (i.e. Q1, Q2, Q3, Q4) where sweep

events and burst events are Q4 and Q2 respectively. The relative strength of each quadrant event is determined in 3D using data from both measurement planes and characterized in time using a wavelet analysis.

Results for unheated wall experiments from the vertical plane show that burst (Q2) and sweep (Q4) events are dominant most of the time. These events show an intermittent temporal interaction where Q2 and Q4 appear to alternate, that is burst and sweep events appear to take turns being the strongest detected quadrant event. Q3 when detected as the most dominant event was often a precursor or post-cursor to Q4. Present work is focused on characterizing how this process changes in the presence of wall heating and on characterizing the quadrant events that contain the most kinetic energy.

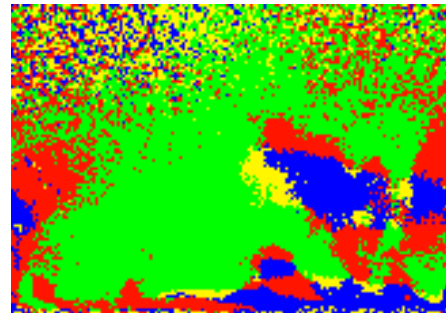


Figure 1: Vertical plane color image showing spatial distribution of quadrant events at $Re_\theta = 1000$. Red = Q1, Blue = Q2, Yellow = Q3, Green = Q4. Mean flow is from left to right in this image.

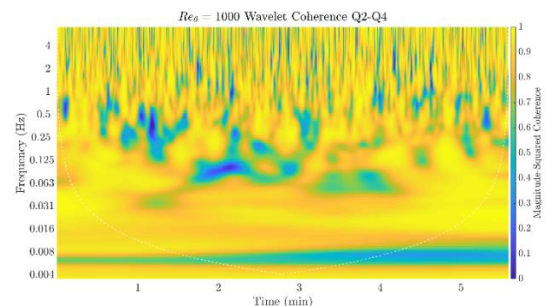


Figure 2: Wavelet coherence diagram for Q2-Q4 events at $Re_\theta = 1000$. Orange and yellow regions correspond to highly coherent wavelet signals.

Kadeem Dennis / kdennis5@uwo.ca
Kamran Siddiqui / ksiddiq@uwo.ca

Energy modelling to determine the feasibility of thermal regulation of aquaculture raceways by utilizing geothermal heat exchange

Aquaculture is a method of fish farming that can decrease the burden on natural habitats and aquatic life populations brought on by the fish capture industry. Raceways are one type of aquaculture system in which aquatic life swims against a current of water, and typically is used for the rearing of salmon or trout. One type of raceway is held within a larger water body, which the water flowing through the raceway is taken from. Seasonal variations in weather can alter the temperature of the water body, and thus the water entering the raceway. Such variation can result in the raceway temperature often being outside of the optimal growth temperature range for most species, causing slowed growth, and death brought on by disease. These lower the economic competitiveness of aquaculture in comparison to fish capture. A method of controlling the aquaculture water temperature must be found to increase the yield and economic competitiveness of the aquaculture industry. This work focuses on a novel approach of using the ground as a heat sink and source to thermally regulate the aquaculture water. The ground provides heating in the winter months, and cooling in the summer months, as the temperature of the soil, beyond a certain depth, is constant throughout the year. Heat exchange is facilitated by vertical borehole heat exchangers with the aquaculture water being passed through the pipes of this system.

Two numerical energy models were developed; one to simulate the heat transfer between the system of geothermal borehole heat exchangers and the ground, and the second to simulate the heat transfer of an aquaculture raceway system based on natural weather conditions as well as the inlet water conditions and ultimately aims to determine the temperature of water inside of the raceway. As the linking of these systems is a novel idea, it was not

known if the idea was feasible. Through the creation and study of these energy models it was determined, for the first time that, it is feasible to regulate the temperature of aquaculture raceways by cycling the raceway water through a system of geothermal vertical borehole heat exchangers. A parametric analysis was conducted on the raceway energy model to determine the effect of certain system parameters on the performance of the system. The two models were then coupled to simulate the thermal regulation of the raceway and results were produced for several global locations. The results show that exchanging heat with the ground is an effective method of thermally regulating an aquaculture raceway in all locations. Comparing the results with the unregulated cases produced increases in the raceway water temperature, in some sites, of up to 200% and decreases in summer months of up to 17%. As a result, the time that the water temperature was within the optimal growth temperature range could increase by 100% - 400% for some species.

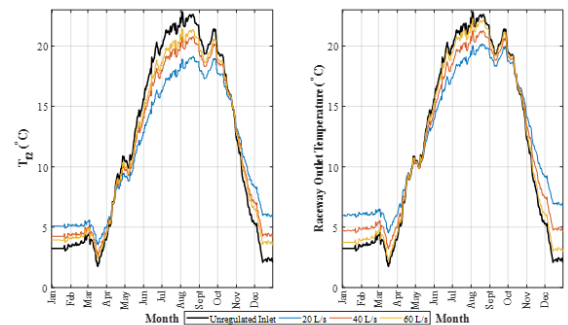


Figure 1: Outlet temperature of 32 geothermal boreholes with 6m borehole spacing (a), and raceway outlet temperature (b) with flow rates of 20, 40, and 60 L/s

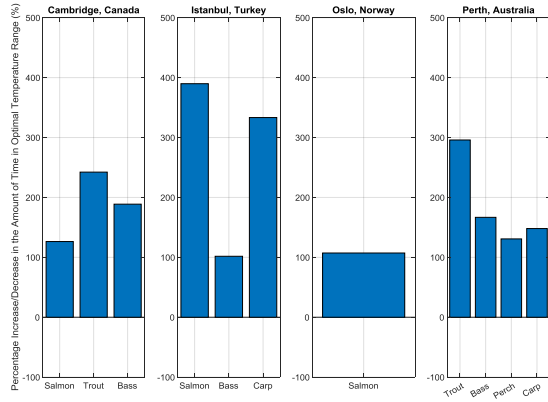


Figure 2: Percentage increase in the yearly time for which the aquaculture raceway is within the optimal growth temperature range for various species at four locations.

Mitchell H. Kuska / mkuska@uwo.ca

Kamran Siddiqui / ksiddiq@uwo.ca

Christopher T. DeGroot / cdegroo5@uwo.ca

Characterizing the formation and dynamics of liquid droplets in a gas turbine afterburner-like configuration

Jet-in-crossflow (JIC) typically involves the injection of a liquid through a simple orifice, into a gaseous crossflow for the purpose of atomizing and mixing the liquid phase amongst the gas. JIC studies have been ongoing for over half a century with interest originating and continuing to be pertinent to aerospace applications. Gas turbine aeroengine afterburners often leverage the simplicity of JIC for fuel injection to reduce part weight and complexity. Prediction of droplet size, distributions, and trajectories has been studied under several conditions including subsonic and supersonic flow, and high and low ambient pressures and temperatures. These background flow conditions and their effect on the behavior on droplet dynamics has been investigated at a global level, however the use of a spray bar for injection and the influence of local structure of gaseous flow on the droplet dynamics has not been investigated.

Combustion instabilities are also of primary concern in the design and operation of aeroengines and other large energy combustions systems. These instabilities behave non-linearly, are difficult to predict and mitigate, and can lead to extensive damage and safety concerns in systems that demonstrate such instabilities. Combustion instability occurs due to the closed-loop coupling of flow instabilities within the system. In an afterburner, flame holder wakes, gas velocity fluctuations at the gas turbine outlet, and certain boundary conditions promote combustion instability. Boundary conditions and system geometric parameters are a design specific source of non-linearity, and so it is desirable to investigate the effect of flow instabilities to address the overall instability.

It has been reported in the literature that bulk gas velocity fluctuations are related to fluctuations in the

heat released by combustion. However, such a relation is primarily observed through bulk parameterization using empirical relations. There is a lack of detailed experimental studies investigating these processes at a local level.

The objective of this research is therefore to characterize turbulent gas flow in a typical afterburner configuration, and to examine the effects of local turbulent structures on the behavior of liquid fuel droplets created by jet-in-crossflow fuel injection.

Experiments are performed in a wind tunnel with a 27cm by 27cm test section, 69cm long with walls made of clear acrylic for flow visualization. Simulated fuel is injected through a 0.8mm orifice in a 4mm spray bar. This JIC spray is investigated for a range of momentum flux ratios, defined as the ratio of fluid-to-gas kinetic energy. To simulate afterburner configuration, a bluff body is used to examine the effects of the flame holder on the fuel droplet dynamics.

In addition to flow instabilities, combustion instabilities can result due to acoustic coupling within the system. The effect acoustic behaviors on fuel droplet advection is also of interest.



Figure 1: Wind tunnel contraction and test section containing a 4mm spray bar



Figure 2: Spray bar (4mm dia.) with 0.8mm injection orifice

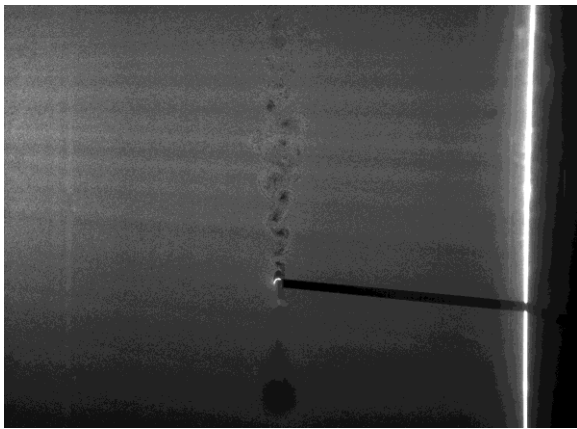


Figure 3: Particle image velocimetry images of the spray bar wake

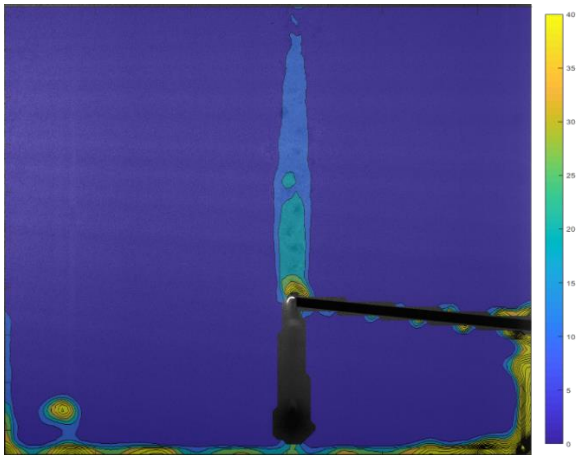


Figure 4: Streamwise turbulent intensity overlaid on the particle image velocimetry image of the spray bar wake. Freestream turbulence intensity < 1.5%

Matthew D. Mahaffy / mmahaffy@uwo.ca
Kamran Siddiqui / ksiddiq@uwo.ca

Characterizing convective heat transfer in PCM-based latent thermal energy storage systems

As the global energy demand rises, our use of fossil fuels also increases since alternative sources of energy are not yet developed enough to be an effective replacement. However, implementation of energy storage can reduce fossil fuel dependence. Energy that would be wasted can be stored until it can be used and therefore conserved reducing the total demand. Surplus energy from intermittent renewable sources could be stored to improve the equalization of supply and demand, making renewable sources more competitive.

Heat is a convenient form to store energy since a large fraction of energy is converted to heat for end-use. Latent-heat systems, which take advantage of the large energy capacity associated with freezing and melting of a material, have a lot of advantages over systems that simply rely on change in temperature; however, the “phase change materials” (PCMs) used in these systems have very low thermal conductivity, which makes heat transfer to the solid phase very difficult. The mechanisms of phase change are also complicated, involving changes in volume and density between phases as well as changing the dominant method of heat transfer from conduction to convection and vice-versa.

Experimental investigations into the fundamental physics of heat transfer are being conducted by the authors. In order to fully characterize the heat transfer, both temperature and velocity data are required. The velocity data is captured using “particle image velocimetry” (PIV) a non-invasive technique whereby a sheet of laser light is introduced to seed particles embedded in the PCM. Images are taken capturing the position of these particles over time, giving the velocity of the flow with high spatial resolution. An existing technique is being applied to non-invasively measure the temperature of the PCM using the same laser and a fluorescent dye with is sensitive to temperature, called “laser-induced

fluorescence” which to our knowledge has not been applied to PCM before.

One promising method to enhance heat transfer to PCMs is using porous-media filled with PCM. Large systems such as this are hard to model since the small-scale behaviour is unknown. A pore-scale model has been developed and tested. Results show that convective flow patterns have a significant influence on the heat transfer behaviors at the surface and on the melting rate and pattern of the PCM.

Another popular method of enhancing heat transfer to PCMs is using a finned heat transfer surface. An experimental setup to investigate this geometry is currently under development.

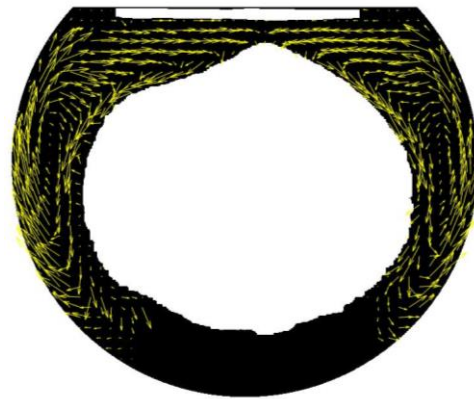


Figure 1: An example flow velocity field at the pore-scale



Figure 2: A photo of an experimental setup being developed to characterize heat transfer to PCM from fins

Kyle Teather / kteather@uwo.ca
Kamran Siddiqui / ksiddiqui@uwo.ca

Publications

1. Ashton, R., Refan, M., Iungo, V., Hangan, H., 2019. "Wandering corrections from PIV measurements of tornado-like vortices". *Journal of Wind Engineering and Industrial Aerodynamics*, 189, 163-172.
2. Hangan, H., Romanic, D., Jubayer, C., 2019. "Three-dimensional, non-stationary and non-Gaussian (3D-NS-NG) wind fields and their implications to wind-structure interaction problems". Accepted for publication *Journal of Fluids and Structures*.
3. Hassanzadeh, A., Naughton, J.W., LoTufo, J., Hangan, H., 2019. "Aerodynamic load distribution and wake measurements on a sub-scale wind turbine". *Journal of Physics. Conference Series*.
4. Jubayer, C., Romanic, D., Hangan, H., 2019. "Aerodynamic loading of a typical low rise building for an experimental stationary and non-Gaussian impinging jet". *Wind & Structures* 28: 315-329.
5. Junayed, C., Jubayer, C., Parvu, D., Romanic, D., Hangan, H., 2019. "Flow field dynamics of large-scale experimentally produced downburst flows". Submitted to *Journal of Wind Engineering and Industrial Aerodynamics*. 188, 61.
6. Karami, M., Hangan, H., Carassale, L., Peerhossaini, H., 2019. "Coherent structures in tornado-like vortices". *Physics of Fluids*, accepted as Editor's cover pick.
7. Romanic, D., LoTufo, J., Hangan, H., 2019. "Transient behavior in impinging jets in crossflow with application to downburst flows". *Journal of Wind Engineering and Industrial Aerodynamics* 184: 209-227.
8. Elshaer, A., Bitsuamlak, G.T., Abdallah, H., 2019. "Progressive damage aerodynamics for low-rise buildings". *Wind and Structures*, 28, 389-404.
9. Gairola, A., Bitsuamlak, G.T., 2019. "Numerical tornado modeling for a common interpretation of experimental simulators". *Journal of Wind Eng. & Industrial Aerodynamics* 186, 32-48.
10. Khasay, M.T., Bitsuamlak, G.T., Tariku, F., 2019. "Effect of exterior convective heat transfer on high-rise building energy consumption". *Building Simulation*.
11. Zhao, Z., Dai, K., Camara, A., Bitsuamlak, G.T., Sheng, C., 2019. "Wind turbine tower failure modes under seismic and wind loads". *Journal of Performance of Constructed Facilities* 33(2).
12. Bezabeh, M.A., Bitsuamlak, G.T., Popovski, M., Tesfamariam, S., 2018. "Probabilistic serviceability-performance assessment of tall mass-timber buildings subjected to stochastic wind loads: Part I-structural design and wind tunnel testing". *Journal of Wind Engineering and Industrial Aerodynamics* 181: 85-103.
13. Bezabeh, M.A., Bitsuamlak, G.T., Popovski, M., Tesfamariam, S., 2018. "Probabilistic serviceability-performance assessment of tall mass-timber buildings subjected to stochastic wind loads: Part II-structural reliability analysis". *Journal of Wind Engineering and Industrial Aerodynamics* 181: 112-125.

14. Bezabeh, M.A., Gairola, A., Bitsuamlak, G.T., Popovski, M., Tesfamariam, S., 2018. "Structural performance of multi-story mass-timber buildings under tornado-like wind field". *Engineering Structures* 177: 519-539.
15. Elshaer, A., Bitsuamlak, G.T., 2018. "Multi-objective aerodynamic optimization of tall building openings for wind-induced load reduction". *Journal of Structural Engineering* 144 (10).
16. Enajar, A.F., Jacklin, R.B., El Damatty, A.A., 2019. "Nonlinear modeling of roof-to-wall connections in a gable-roof structure under uplift wind loads". *Wind and Structures, an International Journal*, 28: 181-190.
17. Ibrahim, I., El Damatty, A.A., Elawady, A., 2019. "The dynamic effect of downburst wind field characteristics on the longitudinal forces on transmission towers". *Frontiers in Built Environment* 5 (59).
18. Elawady, A., El Damatty, A.A., 2018. "Longitudinal forces on transmission towers due to non-symmetric downburst ground wire loads". *Special ASCE Publication*.
19. Fadlallah, H., Jarrahi, M., Herbert, É., Ferrari, R., Méjean, A., Peerhossaini, H., 2019. "Active fluids: effects of hydrodynamic stress on growth of self-propelled fluid particles". *Journal of Applied Fluid Mechanics*.
20. Habchi, C., Ghanem, A., Lemenand, T., Della Valle, D., Peerhossaini, H., 2019. "Mixing performance in split-and-recombination milli-scale mixers- a numerical analysis". *Chemical Engineering Research & Design*, 142, 298-305.
21. Karami, M., Hangan, H., Carassale, L., Peerhossaini, H., 2019. "Coherent structures in tornado-like vortices". *Physics of Fluids*. 31:8.
22. Bashar, M., Siddiqui, K., 2018. "Experimental investigation of transient melting and heat transfer behavior of nanoparticle-enriched PCM in a rectangular enclosure". *Journal of Energy Storage* 18: 485-497.

Conferences

1. Ashrafi A., Romanic D., Hangan H., "Flow properties for a large scale tornado-like vortex", The 15th International Conference on Wind Engineering, Beijing, China. September 2019
2. Romanic D., Shoji H., Hangan H., "Dynamic structural analysis of scaled lighting pole model in physically simulated tornadic flow", FSSIC Symposium on Fluid-Structure-Sound Interactions and Control, Crete Island, Greece. August 2019
3. Hangan, H., "Non Synoptic Winds; from Nature to Engineering", National Wind Engineering Conference (NWECC 2), Bucharest, Romania. June 2019. Guest Speaker
4. Hassanzadeh, A., Naughton, J.W., LoTufo, J., Hangan, H., "Fabrication and testing of a sub-scale wind turbine blad", Wind Energy Science Conference (WESC-19), Cork, Ireland. June 2019
5. Jubayer C., Vickery P., Hangan H., Banik S., "Wind loads on low-rise buildings in tornado-like vortices", The joint Canadian Society for Mechanical Engineering and CFD Society of Canada International Congress, London, Canada. June 2019
6. Karami M., Hangan H., Carassale L., Peerhossaini H., "Relationship between POD modes and physical mechanisms in tornado-like vortex", The joint Canadian Society for Mechanical Engineering and CFD Society of Canada International Congress, London, Canada. June 2019
7. Kassab A., Vickery P., Jubayer C., Banik S., Hangan H., "Tornado-induced internal and external pressures on a low-rise building with multiple openings", The joint Canadian Society for Mechanical Engineering and CFD Society of Canada International Congress, London, Canada. June 2019
8. Ashrafi A., Romanic D., Chowdhury C., Hangan H. "Producing 1/100 and larger scale tornadoes in a wind simulator", Tornado Hazard Wind Assessment and Reduction Symposium (THWARTS 2018), Champaign, USA. September 2018
9. Burlando M., Romanic D., Hangan H., Solari G., "Wind tunnel experimentation on stationary downbursts at WindEEE", XV Conference of the Italian Association for Wind Engineering (IN-VENTO 2018), Napoli, Italy. September 2018.
10. Hangan, H., "Identifying and stimulating broader stakeholder involvement", International Conference on Research Infrastructure, Vienna, Austria. September 2018. Panel Member
11. Romanic D., Hangan H., "The interplay between background atmospheric boundary layer winds and downburst outflows. A first physical experiment". XV Conference of the Italian Association for Wind Engineering (IN-VENTO 2018), Napoli, Italy. September 2018.
12. Bezabeh, M. A., Bitsuamlak G., Tesfamariam, S. "Probabilistic serviceability-performance assessment of tall mass-timber buildings subjected to stochastic wind loads", CSCE 2019 – Structural Engineering, Laval, Canada. June 2019.

13. Geleta, T., Gairola, A., Abdallah, H., Bitsuamlak G.T., “Hindcasting the damage of Ottawa-Gatineau tornado outbreak of September 2018: a coupled CFD and FEA computational approach”, CSCE 2019 – Structural Engineering, Laval, Canada. June 2019
14. Bitsuamlak G.T., “AI-assisted climate-resilient and sustainable architectural design” AI Government Summit, Toronto, Canada. October 2018. Keynote speaker
15. Kahsay, M., Bitsuamlak, G.T., Tariku, F., “Influence of external shading on convective heat transfer of high-rise buildings”, Building Performance Analysis Conference and Sim-Build co-organized by ASHRAE and IBPSA-USA, Chicago, USA. September 2018.
16. El Damatty A.A., Ezami N., Hamada A., “Case study for behavior of transmission line structures under full-scale flow field of Stockton, Kansas, 2005 Tornado”, ASCE Electrical Transmission and Substation Structures, Atlanta, USA. November 2018.
17. El Damatty A.A., Shehata A., Enajar A., Rosenkrantz J., El Ezaby F.Y., “Research for adaptive and sustainable structures”, 8th International Conference on Environmental Effects on Buildings and People: Actions, Influences, Interactions, Discomfort, Cracow, Poland. October 2018. Keynote Lecture
18. El Damatty A.A., El Ezaby F.Y., “The integration of wind and structural engineering”, The World Congress on Advances in Civil, Environmental & Materials Research (ACEM18) Songdo Convensia, Incheon, Korea. August 2018. Keynote Lecture
19. Nguyen M.C., Jarrahi M., Salek M., Peerhossaini H., “Control of particle distribution at the outlet of a double Y-microchannel using pulsatile flow”, The ASMEJSME-KSME Joint Fluids Engineering Conference, San Francisco, United States. July 2019.
20. Vourc'h T., Leopoldes J., Peerhossaini H., “Phototactic behaviour of active fluids: effects of light perturbation on diffusion coefficient of bacterial suspensions”, The ASME-JSME-KSME Joint Fluids Engineering Conference, San Francisco, United States. July, 2019. Invited speaker
21. Karami M., Hangan H., Carassale L., Peerhossaini H., “Relationship between POD modes and physical mechanisms in tornado-Like vortex”, The Joint Canadian Society for Mechanical Engineering and CFD Society of Canada International Congress, London, Canada. June, 2019.
22. Habibi Z., Vourc'h T., Leopoldes J., Mehdizadeh-Allaf M., Peerhossaini H., “Mechanics of active fluids at a solid liquid Interface: diffusion of synechocystis Sp. Pcc 6803 in dilute regime”, The Joint Canadian Society for Mechanical Engineering and CFD Society of Canada International Congress, London, Canada. June 2019.
23. Dennis, K., Siddiqui, K., “Characterization of thermals in a heated turbulent boundary layer”, ASME-JSME-KSME Joint Fluids Engineering Conference, San Francisco, United States. July 2019
24. Dennis, K., Siddiqui, K., “Investigation of turbulent flow in a heated boundary layer”, ASME-JSMEKSME Joint Fluids Engineering Conference, San Francisco, United States. July 2019

25. Islam, A., Toxopeus, K., Siddiqui, K., “The influence of thermal storage inserts on the microalgae growth rate in a photobioreactor for Biofuel Production”, European Conference on Sustainability, Energy and Environment, Brighton, United Kingdom. July 2019.
26. Dennis, K., Siddiqui, K., “Three-dimensional characterization of bursting and sweeping phenomena in the turbulent boundary layer”, Joint Congress of the Canadian Society for Mechanical Engineering and CFD Society of Canada, London, Canada. June 2019.
27. Gadallah, A., Siddiqui, K., “Generation of self organized bubble train flow”, Joint Congress of the Canadian Society for Mechanical Engineering and CFD Society of Canada, London, Canada. June 2019.
28. Kuska, M., DeGroot, C., Siddiqui, K., “Utilizing geothermal looping for thermal regulation of an aquaculture pond”, Joint Congress of the Canadian Society for Mechanical Engineering and CFD Society of Canada, London, Canada. June 2019.
29. Teather, K., Siddiqui, K., “Characterization of transient flow velocities during melting of PCM in a uniformly heated circular cavity”, Joint Congress of the Canadian Society for Mechanical Engineering and CFD Society of Canada, London, Canada. June 2019.
30. Teather, K., Siddiqui, K., “Experimental study of natural convection in a horizontal uniformly heated cylinder”, Joint Congress of the Canadian Society for Mechanical Engineering and CFD Society of Canada, London, Canada. June 2019.
31. Siddiqui, K., “Clean energy and sustainability: keys to future prosperity”, 9th International Mechanical Engineering Conference, Karachi, Pakistan. March 2019. Invited Speaker

Grants

Mitacs Accelerate & Institute for Catastrophic Loss (ICLR) / \$110,000 / 2019-2020

Tornado Hazards and Exposure Model for Canadian Communities

Hangan, H.

Tornadic Loads Research with FM Global Phase3 / \$71,400 USD / 2019-2020

Chowdhury, J., Romanic D., Hangan H.

Performance test of HVAC unit of Bluewater Technology / \$7,500 / 2019

Chowdhury, J., Hangan, H.

S2E London, Ontario Development / \$25,000 / 2019

Optimal Orientation for Pedestrian Level Wind Comfort and Mitigation Snow Drift for S2E Development.

Chowdhury, J., Bitsuamlak G.T., Hangan, H.

Regional Power – Long Lake Hydroelectric Project / \$57,300/ 2019-2021

Hangan, H.

Applied Research Associates, Inc. / \$ 152,000 USD / 2018-2019

Development of Tornado Design Criteria for Buildings and Shelters Subject to Tornado Induced Loads

Hangan, H.

ImpactWx / \$ 130,750 / 2018

Hangan, H.

S2E London, Ontario Development / \$25,000 / 2019

Optimal Orientation for Pedestrian Level Wind Comfort and Mitigation Snow Drift for S2E Development

Chowdhury, J., Bitsuamlak G.T., Hangan, H.

Next Tracker / \$15,000 / 2019

Solar System Aeroelastic Testing Review

Bitsuamlak, G.T.

Compute Canada / \$7,683 / 2019-2020

Climate Resilience and Sustainable Cities of Tomorrow. Computational Resources Allocation

Bitsuamlak, G.T.

Natural Sciences & Engineering Research Council of Canada (NSERC) Discovery Accelerator / \$ 120,000 / 2018-2020

Novel Computational and Experimental Wind Engineering Approaches for Community Level Performance Assessment

Bitsuamlak, G.T.

Natural Sciences & Engineering Research Council of Canada (NSERC) Discovery / \$120,000 / 2018-2020

Department of National Defense Supplement Award

Novel Computational and Experimental Wind Engineering Approaches for Community Level Performance Assessment

Bitsuamlak, G.T.

The Centre for Energy Advancement through Technological Innovation (CEATI) / \$56,000 / 2019-2020

Performance Assessment of Transmission Line Structures under Downbursts and Tornadoes

El Damatty, A. A.

Ontario Centres of Excellence (OCE) VIP1 and Centric Engineering / \$ 20,000 / 2018-2019

Assessment of Application Heavy Timber Construction for Low-Rise Buildings

El Damatty, A. A., Hamada, A.

Natural Sciences & Engineering Research Council of Canada (NSERC) Engage / \$25,000 / 2018-2019

Assessment of Application Heavy Timber Construction for Low-Rise Buildings

El Damatty, A. A.

The National Natural Science Foundation of China (NSFC) / \$458,000 / 2018-2020

Effects of Tornado and Downbursts on Network-like Infrastructures

Yang, Q., El Damatty, A.A., Backer, C.

Western University Start-Up / \$ 300,000 / 2018-2022

Peerhossaini, H.

Natural Sciences & Engineering Research Council of Canada (NSERC) / \$ 195,000 / 2018-2023

Characterization and Development of PCM-based Thermal Energy Storage Systems

Siddiqui, K.

National Research Council Canada (NRC) Ottawa, ON / \$40,000 / 2018-2020

Characterization of the Afterburner Spray Performance

Siddiqui, K.

Honors and Awards

2019 Honors and Awards

Doctor Honoris Causa – University of Construction. Bucharest, Romania
Hangan, H.

Invited Professor, Short Course, Wind Engineering: Classical and New Concepts, Universidad de Granada, Spain
Hangan, H.

Invited speaker, Physics Colloquium, Western University
Bitsuamlak, G.T.

Invited Keynote Speaker, Wood Rise 2019 Conference, Quebec, Canada.
Bitsuamlak, G.T.

Invited Speaker, Wind-resilient and Sustainable Architectural Engineering. University of Michigan
Bitsuamlak, G.T.

Invited Speaker, Synoptic and Non-Synoptic Wind Loading on Buildings. Stephenson, Engineering Inc.
Bitsuamlak, G.T.

Invited Speaker, Computational Wind Engineering and Building Science, Theakston Environmental Inc.
Bitsuamlak, G.T.

Invited Speaker, A Community Outreach. Mr. Ken Whitnall Residence
Bitsuamlak, G.T.

Keynote Speaker, Certificate Presentation Ceremony, Professional Engineers of Ontario
El Damatty, A.A.

Invited Visiting Professor, Seoul National University, Seoul, Korea
El Damatty, A.A.

Chair Professor, South China University of Technology, Guangzhou, China
El Damatty, A.A.

High-End Foreign Expert, Sichuan University, China
El Damatty, A.A.

Invited Keynote Speaker, the 2nd International Conference on Civil Engineering and Architect (ICCEA). Seoul, Korea.
El Damatty, A.A.

Invited Keynote Speaker, the 2019 International Conference on Engineering Education and Innovation (ICEEI), Seoul, Korea.

El Damatty, A.A.

Invited Keynote Speaker, The ASME-JSME-KSME Joint Fluids Engineering Conference. San Francisco, USA
Peerhossaini, H.

Invited Keynote Speaker, Joint Conference of the Canadian Society for Mechanical Engineering and CFD Society of Canada. London, Canada
Peerhossaini, H.

Invited Speaker, Urban Climate Change Resilience: in Quest of a Theory for Adaptive Change. Western Civil Engineering Seminar, London, Canada.
Peerhossaini, H.

Invited Speaker, 9th International Mechanical Engineering Conference. Karachi, Pakistan.
Siddiqui, K.

2018 Honors and Awards

Best Journal Paper Award, American Association for Wind Engineering
Hangan, H.

Invited Professor, Institute de Mécanique des Fluides, Toulouse, France
Hangan, H.

Short Course, Novel Techniques in Wind Engineering, University of Genova, Genova, Italy
Hangan, H.

Member, European Research Council International Advisory Board for Project THUNDERR
Hangan, H.

Invited Keynote Speaker, International Union of Theoretical and Applied Mechanics Symposium on Critical Flow Dynamics Involving Moving/Deformable Structures with Design Applications, Santorini, Greece
Hangan, H.

Keynote speaker, AI Government Summit, Re-work. Toronto
Bitsuamlak, G.T.

Keynote Panel Member, Inaugural Research Western Conference
Bitsuamlak, G.T.

NSERC Discovery Accelerator Supplement (DAS) Award
Bitsuamlak, G.T.

NSERC Discovery Department of National Defense (DND) Supplemental Award
Bitsuamlak, G.T.

Faculty Scholar, Western University
Bitsuamlak, G.T.

Associate Fellow, Ethiopian Academy of Science
Bitsuamlak, G.T.

Faculty Scholar, Western University
Bitsuamlak, G.T.

Ontario Professional Engineers Engineering Medal for Research and Development
El Damatty, A.A.

Invited Keynote Speaker, 8th International Conference on Environmental Effects on Buildings and People-Actions, Influences, Interactions, and Discomfort. Cracow, Poland
El Damatty, A.A.

Invited Keynote Speaker, 15th International Conference on Structural and Geotechnical Engineering. Ain Shams University, Egypt
El Damatty, A.A.

Invited Keynote Speaker, 14th Arab Structural Engineering Conference, Irbid, Jordan
El Damatty, A.A.

Events

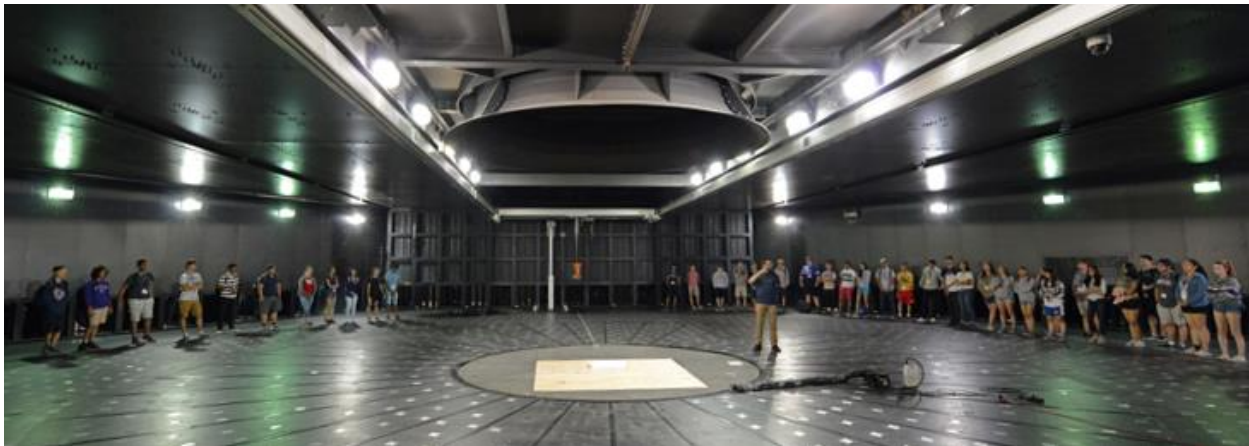
SHAD at WindEEE

Western University is the latest top university to join with SHAD, a prestigious program which brings the best and the brightest high school students to university campuses across the country every July for an intense program that helps them reach their full potential. SHAD, founded in 1980, has become known as an incubator for innovation and entrepreneurship among these students who specialize in STEM (Science, Technology, Engineering and Math). With an impressive list among its 15,000 alumni which includes 30 Rhodes Scholars, SHAD has seen a record number of applications for two years straight.

Western becomes the 12th host university campus around the country for the one-month residential program with places highly sought after by students who go through a rigorous competition and application process.

Each year, the program has a specific theme, built around a current economic and social problem. The students collaborate to develop a unique innovative product or service that addresses the issue. As part of this engineering and design challenge, teams are taught how to build a business and marketing plan, and design and build working prototypes. Winning projects advance to national judging and results are celebrated each fall.

A typical day at SHAD includes experiential learning, from class to labs and beyond. Students are inspired by university professors, business leaders, entrepreneurs and innovators, who help them set aspirational goals and envision their own extraordinary potential.



This summer, WindEEE Research Institute had the privilege to be one of Western's hosts for the SHAD group. The day at WindEEE started with a presentation about the Dome's capabilities, followed by facility tour and a tornado simulation.

A technical presentation on wind turbine designs and technologies introduced the students to the hands-on session. The students, divided in groups, designed and assembled small wind turbines to be tested inside the WindEEE test chamber. With plenty of construction materials at hand and keeping the rules of the game to a minimum, it did not take long until the innovative prototypes were ready to be tested. The competition was equally fun and exciting, bringing everything from entertaining failures to amazing performances.

Western Formula Racing Unveiling

Western Engineering students are among the most active students on campus when it comes to extracurricular activities, participating in faculty-based groups, clubs and teams. The Western Formula Racing (WRF) team is for students who are interesting in all things automotive and would like to become involved in the world of Formula SAE cars. Students use their engineering skills along with university and external resources available to them to fabricate and compete a formula-style race car in an annual competition with approximately 120 other vehicles from colleges and universities around the world.



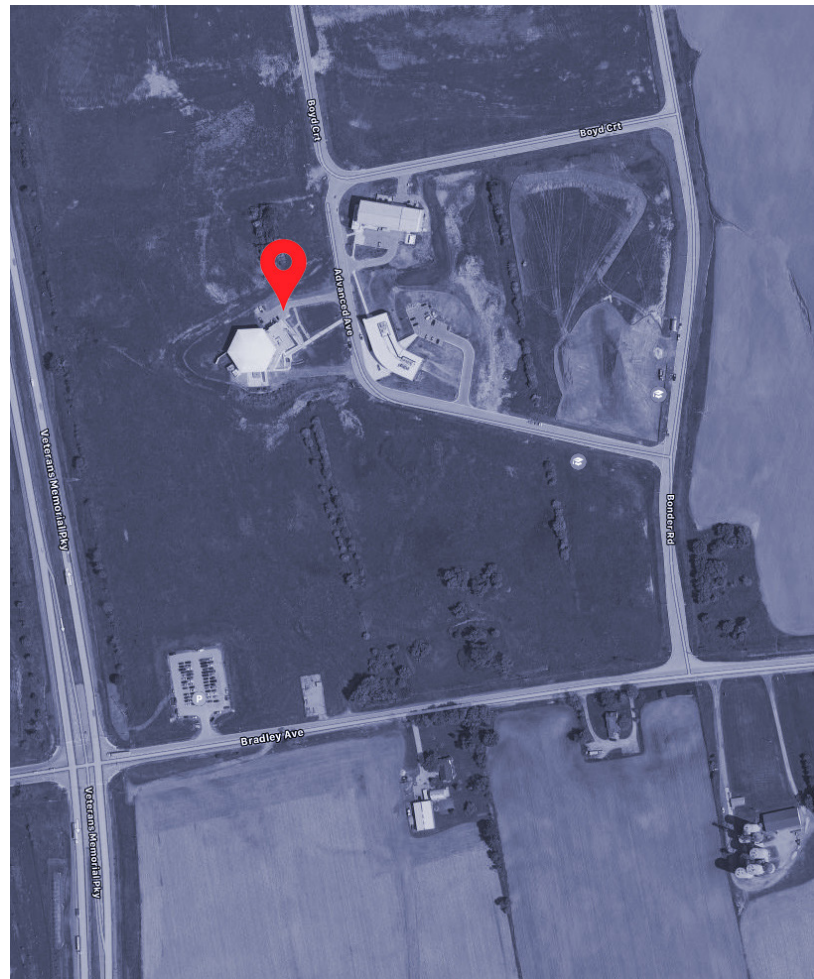
WindEEE's involvement in the WRF this year was both in the areas of fabrication and presentation. In recent years, WindEEE has donated foam and services to fabricate cores to make wing elements for the car. This year was no exception as design became reality when the WindEEE team used its CNC hot wire foam cutter to make eight cores for wings on the car.

Following the final assembly of the car, an amazing opportunity arose from the team's need to host an unveiling event worthy of all their hard work. The futuristic look and presentation capabilities of WindEEE, along with its uniquely large testing chamber, made it the perfect place to host roughly 90 attendees for the 30th anniversary of the WRF car unveiling. A day full of laughs, alumni presentations, cinematic experiences and testing out the team's driving simulator had everyone at the event excited for what next year would have in store.

**WinDEEE Research Institute
Western University**

**2535 Advanced Avenue
London, ON N6M-0E2
Canada**

**t: +1 (519) 661-2111 x89143
f: +1 (519) 661-3339
windeee@uwo.ca
www.windeee.ca**



**WinDEEE Research Institute
Western University**

**2535 Advanced Avenue
London, ON N6M-0E2
Canada**

T: +1 (519) 661-2111 x89143

F: +1 (519) 661-3339

windeee@uwo.ca

www.windeee.ca